Research Square

Preprints are preliminary reports that have not undergone peer review.
They should not be considered conclusive, used to inform clinical practice,
or referenced by the media as validated information.

A novel mixed-variable beam element and its application on the free vibration of Timoshenko beam

Lv Ding
Suzhou University of Science and Technology
Xue Xia
Suzhou University of Science and Technology
Siyuan Bao
bsiyuan@usts.edu.cn
Suzhou University of Science and Technology
S D Wang
Oklahoma State University

Research Article

Keywords:

Posted Date: November 5th, 2026

DOI: https://doi.org/10.21203/rs.3.rs-11226309/v1

License: This work is licensed under a Creative Commons Attribution 4.0 International License.
Read Full License

Additional Declarations: No competing interests reported.

A novel mixed-variable beam element and its application on the free vibration of Timoshenko beam

Lv Ding[1], Xue Xia[1], Siyuan Bao[1]*, Shuodao Wang[2]*

[1]*School of Civil Engineering, Suzhou University of Science and Technology, Suzhou 215011, Jiangsu, China*

[2]*School of Mechanical and Aerospace Engineering, Oklahoma State University, Stillwater, Oklahoma, 74078, USA*

* Corresponding author's email: bsiyuan@usts.edu.cn, shuodao.wang@okstate.edu

Abstract: In the framework of mixed-variable finite element method, this paper proposes a new 2-node 8-degree-of-freedom Timoshenko beam element. The nodal degrees of freedom of this novel element are constructed based on the transverse displacement of the beam, the cross-sectional rotation, and the internal forces, namely the shear force and bending moment. Though the transverse displacement field and the cross-sectional rotation field are mutually independent in the Timoshenko beam, two novel displacement field expressions that respectfully correspond to the transverse displacement and cross-sectional rotation of the Timoshenko beam element is proposed based on the cubic Hermite interpolation function. The two displacement fields are synergistically used to describe the vibration characteristics of the beam element, then the stiffness and mass matrices of the element are derived and the natural frequencies of a Timoshenko beam are solved. Free vibration analyses are conducted by using the proposed beam element with different meshes under three typical boundary conditions. Through comparison with the existing results, the advantage of the proposed finite element in computational accuracy is verified, whose error is normally half of or less than that of the conventional Timoshenko beam element with the same interpolation order of the shape function. Further, the internal forces at the nodes are directly obtained together with the displacements in the solving process as the shear force and bending moment are naturally and reasonably composed into the nodal freedoms. The precision of the internal force by the proposed element is also high in that the distribution of the shear force and the bending moment obtained is consistent with the analytical results. The numerical analysis demonstrates the efficiency of the presented novel element together with excellent precision for nodal internal forces. The predicted results by the proposed element are expected to serve as benchmarks for evaluating the performance of other numerical methods.

0. Introduction

With engineering structures evolving toward high performance, lightweight, and multi-scale designs, beam-like components have been widely applied in fields such as aerospace, marine, and civil engineering. In the vibration response analysis of beams, two basic theories are commonly utilized: the Euler-Bernoulli beam theory and the Timoshenko beam theory. Although numerous scholars have analyzed and constructed various models based on the Euler-Bernoulli beam theory, it tends to neglect transverse shear deformation effects (where the cross-sectional normal remains perpendicular to the neutral axis), making it highly susceptible to the shear locking phenomenon. To address this, Timoshenko beam theory introduces an independent cross-sectional rotation variable, allowing the cross-section to rotate relative to the neutral axis. Consequently, the local slope of the transverse displacement is not generated solely by bending, but also incorporates actual shear strain, thereby effectively accounting for the influences of both shear deformation and rotary inertia. Concurrently, in numerical analyses based on the Timoshenko beam, the finite element method (FEM) and the formulation of shape functions exert a decisive impact on computational accuracy.

As research about Timoshenko beam elements deepens, finite element methods considering shear deformation effects have been developed rapidly. Among the finite element formulations, a relatively simple and representative model is the linearly interpolated Timoshenko beam element proposed by Hughes [1] in 1977. Although this element has a concise form, its bending moment and curvature within the element are formulated as constants. As a result, a highly refined mesh is often required to achieve high computational accuracy, and it is prone to shear locking, which severely restricts its practical utility in model construction. However, Przemieniecki [2] considered the bending and shear deformation effects separately based on theoretical displacement differential equations, where a cubic interpolation function is adopted for the transverse deflection displacement field, while a quadratic interpolation function is used for the rotation displacement field. Under normal circumstances, the resulting stiffness matrix can essentially be regarded as the exact stiffness matrix of the element, offering high computational accuracy and a certain degree of versatility.

Building upon this, Friedman [3] proposed a beam element model based on the Timoshenko generalized displacement beam theory. This method assumes a cubic interpolation for transverse displacement and a quadratic interpolation for rotation displacement by requiring them to satisfy the two homogeneous differential equations associated with Timoshenko's beam theory. By deriving the displacement shape functions of the beam element and establishing the standard form for beam element

interpolation functions, thereby the stiffness equation can be obtained by Hamiliton principle. For curved shear deformable beams, similar finite element [4] is established, where the element formulation is based on shape functions that satisfy the corresponding homogeneous form of the partial differential equations of motion which renders it free of shear and membrane locking. Nevertheless, this approach requires solving the homogeneous differential equations within Timoshenko's beam theory, making the process quite cumbersome. Using different establishing approaches, researchers have conducted extensive studies around other interpolation forms of beam elements. For example, Oral [5] proposed a higher-order isoparametric hybrid Timoshenko beam element, assuming a quadratic parabolic interpolation for displacement and a linear interpolation for rotation. Cailleriea et al. [6] present a Timoshenko finite element straight beam with internal degrees of freedom suitable for nonlinear material problems in geomechanics, in which cubic shape function is used for the transverse displacements and quadratic function for the rotations.

In recent years, significant innovations and breakthroughs have been made in Timoshenko beam theory and applications. Gerlach et al. [7] presented an analytical beam element model (ABM) for Timoshenko beam which is used to correctly predict the stator's vibration behavior, in which ABM offers an alternative to the finite element method and to classical analytical models. Zhao et al. [8-9] established Bernoulli-Euler and Timoshenko beam models based on the modified strain gradient elasticity theory. Li et al. [10] made comment on nonlocal effects in nano-cantilever beams. Vibration or stability analysis about nanobeams have been studied, for example, FG piezoelctric nanobeams[11], piezoelectric seiconductor nanobeam [12], analysis of the shear boundary layer adjacent to the bi-material interface based on a modified gradient elasticity theory [13], buckling solutions of FGM nonlocal beam [14], and Finite element formulation of metal foam microbeams [15].

As modern materials increasingly incorporate microstructural configurations, a major advancement has emerged in micromorphic beam theories. A significant theoretical milestone in modeling micromorphic beams was achieved by Challamel et al. [16-17], and they established a connection between micromorphic beam theory and the nonlocal strain gradient theory of Timoshenko beams. Concurrently, Eremeyev and Elishakoff [18] extended this connection to account for rotary inertia effects in micromorphic Euler-Bernoulli and Timoshenko beams. El-Borgi et al. [19] also proposed an analytical Timoshenko beam model merging micromorphic and nonlocal strain gradient effects, effectively eliminating the ill-posedness issues of existing nonlocal theories under specific boundary conditions. Tuna and Kirca [20] presented an exact solution of bending Euler-Bernoulli and Timoshenko beams based on nonlocal

integral model. Karttunen et al. [21] derived the general closed-form solution to the equilibrium equations of the beam, and a Maclaurin series is presented for the general solution by linking the relationship of the load resultants with the two-dimensional in-plane stress. The solution is presented in terms of discrete finite element (FE) degrees of freedom. Their representation yields the exact shape functions for the corresponding beam element. Dehrouyeh-Semnani et al. [22] gave an exact size-dependent Timoshenko beam element, which contains two forms: one 6-DOF beam element, and the other simplified 4-DOF beam element based on modified coupled stress.

For the FG beams, Hassina et al. [23] used the FEM approach to study the static displacement field components, axial stress and shear stress distribution within the framework first order shear deformation theory (FSDT). Murat Çelik et al.[24]addressed the free vibration characteristics of a functionally graded (FG) shear-deformable Timoshenko beam were investigated analytically by Navier solution and numerically by ABAQUS finite element software. Ruocco and Reddy [25-26] gave the analytical displacement and stress solutions of Timoshenko and Bernoulli beam models, further the comparative analysis with Reddy beam model was carried out. From the perspective of energy finite element method, Xie et al. [27] developed an enhanced EFEA model for tapered beams based on Timoshenko beam theory (Timoshenko-EFEA), which accounts for both bending and shear effects. Chen et al. [28] also used an energy finite element approach for high frequency vibration analysis of beams with axial force.

Evidently, substantial progress has been achieved in the study of Timoshenko beam element vibrations. Meanwhile, the finite element method within numerical computation has been widely adopted by scholars for analyzing the mechanical performance of beam components due to its broad versatility, high accuracy, and superior efficiency. For example, Skrinar [29] presented a closed-form finite element formulation for multi-stepped beams and beams with linearly-varying heights by using principle of virtual work. The cracks are simulated by internal hinges endowed with rotational springs.

However, conventional Timoshenko beam elements contain only two degree of freedoms (DOFs) at each node, i.e., transverse displacement and rotation. Such a shape function configuration can lead to sub-optimal element accuracy. Furthermore, in practical theoretical analysis, interpolation shape functions such as linear, quadratic, or higher-order polynomials are often employed to construct beam elements. Yet, many existing Timoshenko beam elements fail to account for the boundary condition influences of shear force and bending moment within the establishment of the variable field because they only consider displacement, rotation, and shear strain. Consequently, their calculation accuracy is low, and the computational efficiency is to be improved.

Though some new type of p-version finite element, such as Fourier-p element [30], has been proposed and used, which is complicated in the expression form of the displacement field. Therefore, establishing an analytical method that simultaneously possesses the database advantages and addresses these limitations is an urgent work, which is carried out in this study.

To meet the above-mentioned demand, this paper proposes a 2-node 8-DOF Timoshenko beam element. The nodal degrees of freedom for this new element are established based on the beam's nodal transverse displacement, nodal cross-sectional rotation, and their corresponding first derivatives, which can be equivalent with nodal shear force and nodal bending moment. Since the transverse displacement field and the cross-sectional rotation field are mutually independent in Timoshenko beams, two kinds of novel and consistent displacement field expression for deflection and cross-sectional rotation of the Timoshenko beam element are proposed based on cubic Hermite interpolation functions. The two proposed displacement fields synergistically describe the vibration characteristics of the beam element. Then the element stiffness matrix and mass matrix are derived, and the corresponding natural frequencies are solved. The Hermite interpolation approach [31-33] has been used in the finite element analysis of Euler-Bernoulli beam or viscoelastic beam. It should be noted that the proposed beam element employs nodal degrees of freedom that represent internal forces，and the beam element is termed as the fusion Timoshenko beam element in this paper. However, this element is fundamentally different from the classic mixed elements proposed by Taylor and Filippou [34], or the hybrid element by Pian [35-36]. The distinction lies in that the interpolation approaches of the displacement and the internal forces are not independently interpolated via a mixed variational principle. Instead, they are derived and transformed from the exact constitutive relationships between the internal forces and the displacement derivatives.

1. Theoretical basis of the fusion Timoshenko beam element

1.1 Construction of the displacement field for the proposed Timoshenko element

Within the framework of the Timoshenko beam theory, the deformation of a beam is described by the transverse displacement and the cross-sectional rotation. The geometric equations can be expressed as:

$$\kappa = \frac{\partial \varphi}{\partial x} \tag{1}$$

$$\frac{\partial w}{\partial x} = \gamma + \varphi \tag{2}$$

where κ denotes the cross-sectional curvature, w represents the transverse displacement, φ is the cross-sectional rotation, and γ signifies the additional rotation angle induced by shear deformation.

From the corresponding constitutive relationships, the constitutive equations can be obtained. The bending moment-curvature relationship is defined as:

$$M = -EI\frac{\partial \varphi}{\partial x} \tag{3}$$

The relationship between shear force and shear strain is given by:

$$Q = kGA(\frac{\partial w}{\partial x} - \varphi) \tag{4}$$

According to the above geometric and constitutive relations, the direct correlation between the axis rotation and internal forces can be established as follows:

$$\frac{\partial w}{\partial x} = \frac{Q}{kGA} + \varphi \tag{5}$$

From Eq. (5), it is evident that the transverse displacement field and the cross-sectional rotation field in a Timoshenko beam are not independent; However, there is a relationship between them via shear deformation. Therefore, by use of cubic Hermite interpolation functions, we innovatively proposes a consistent displacement field expression for the Timoshenko beam element where the transverse displacement and cross-sectional rotation are tightly coordinated. The expressions for the transverse displacement and the cross-sectional rotation of the beam can be respectively formulated as:

$$\begin{aligned} w &= H_1(\xi)w_1 + H_2(\xi)w_1{}' + H_3(\xi)w_2 + H_4(\xi)w_2{}' \\ &= H_1(\xi)w_1 + H_2(\xi)\left(\frac{Q_1}{kGA} + \varphi_1\right) + H_3(\xi)w_2 + H_4(\xi)\left(\frac{Q_2}{kGA} + \varphi_2\right) \end{aligned} \tag{6}$$

$$\begin{aligned} \varphi &= H_1(\xi)\varphi_1 + H_2(\xi)\varphi_1^{'} + H_3(\xi)\varphi_2 + H_4(\xi)\varphi_2^{'} \\ &= H_1(\xi)\varphi_1 - H_2(\xi)\frac{M_1}{EI} + H_3(\xi)\varphi_2 - H_4(\xi)\frac{M_2}{EI} \end{aligned} \tag{7}$$

where the prime denotes differentiation with respect to the x-coordinate, ξ is the non-dimensional coordinate, i.e., $\xi = x/L$. H_i (in which i=1,2,3,4) is the cubic Hermite interpolation function with the expressions as:

$$\begin{cases} H_1 = 1 - 3\xi^2 + 2\xi^3 \\ H_2 = L\xi\left(1 - 2\xi + \xi^2\right) \\ H_3 = 3\xi^2 - 2\xi^3 \\ H_4 = L\xi\left(\xi^2 - \xi\right) \end{cases} \tag{8}$$

Based on the proposed displacement field expressions, Eq. (6) and Eq. (7) are written as:

$$w = \boldsymbol{N}_w \cdot \{q_1^{(1)}\ q_1^{(2)}\ q_1^{(3)}\ q_1^{(4)}\ q_2^{(1)}\ q_2^{(2)}\ q_2^{(3)}\ q_2^{(4)}\}^T \tag{9}$$

$$\varphi = \boldsymbol{N}_\varphi \cdot \{q_1^{(1)}\ q_1^{(2)}\ q_1^{(3)}\ q_1^{(4)}\ q_2^{(1)}\ q_2^{(2)}\ q_2^{(3)}\ q_2^{(4)}\}^T \tag{10}$$

The expression for the column vector of nodal degrees of freedom (DOFs) at each node is defined as: $\boldsymbol{q}_i^e = [w_i \quad \varphi_i \quad Q_i \quad M_i]^T$ (i=1, 2). Therefore, the nodal displacement vector for the 2-node 8-DOF element, $\boldsymbol{q}^e$, is given by:

$$\boldsymbol{q}^e = [q_1^{eT}\ q_2^{eT}]^{\mathrm{T}} = [w_1\ \varphi_1\ Q_1\ M_1\ w_2\ \varphi_2\ Q_2\ M_2]^{\mathrm{T}} \tag{11}$$

To clearly illustrate the configuration and the physical quantities at each node, the schematic of the proposed 2-node 8-DOF beam element is depicted in Figure 1. As shown, each node possesses four generalized degrees of freedom: the transverse displacement w_i, cross-sectional rotation φ_i, shear force Q_i, and bending moment M_i ($i = 1, 2$).

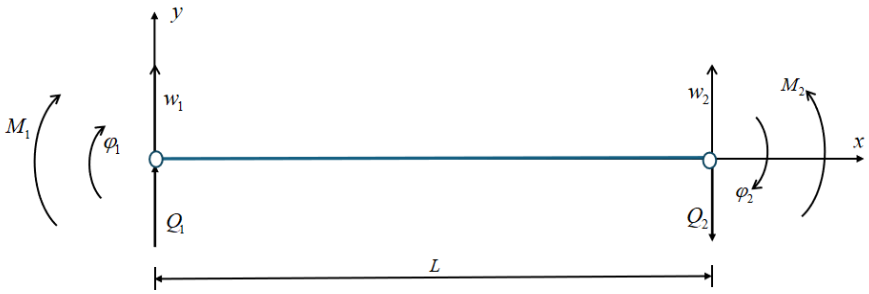


Fig. 1 The present element with nodal degrees of freedom

From Eq.(6), the specific formulations of the corresponding shape functions can be derived as follows:

$$\boldsymbol{N}_w = \left[H_1 \quad H_2 \quad \frac{H_2}{kGA} \quad 0 \quad H_3 \quad H_4 \quad \frac{H_4}{kGA} \quad 0 \right] \tag{12}$$

where $\boldsymbol{N}_w$ represents the shape function matrix for transverse displacement.

From Eq.(7), the shape function matrix $\boldsymbol{N}_\varphi$ for the cross-sectional rotation is:

$$\boldsymbol{N}_{\varphi}=\begin{bmatrix}0 & H_1 & 0 & -\dfrac{H_2}{EI} & 0 & H_3 & 0 & -\dfrac{H_4}{EI}\end{bmatrix} \tag{13}$$

The matrix forms of the transverse displacement and cross-sectional rotation expressions are respectively given by:

$$w=\boldsymbol{N}_{w}\cdot\boldsymbol{q}^{e} \tag{14}$$

$$\varphi=\boldsymbol{N}_{\varphi}\cdot\boldsymbol{q}^{e} \tag{15}$$

Based on the geometric equations, the element strain vector is $\boldsymbol{\varepsilon}=\boldsymbol{B}\cdot\boldsymbol{q}^{e}$, where the strain vector $\boldsymbol{\varepsilon}$ composes of the cross-sectional curvature κ and the additional rotation angle γ induced by shear deformation, and $\boldsymbol{B}$ denotes the strain-displacement matrix composed by $\boldsymbol{B_b}$ and $\boldsymbol{B_s}$. The matrix $\boldsymbol{B_b}$ is the bending strain-displacement matrix and $\boldsymbol{B_s}$ is shear strain-displacement matrix. $\boldsymbol{B_b}$ and $\boldsymbol{B_s}$ are respectively formulated as:

$$\boldsymbol{B}_{b}=\frac{\partial\boldsymbol{N}_{\varphi}}{\partial\xi}\cdot\frac{1}{L} \tag{16}$$

$$\boldsymbol{B}_{s}=\frac{\partial\boldsymbol{N}_{w}}{\partial\xi}\cdot\frac{1}{L}-N_{\varphi} \tag{17}$$

1.2 Natural frequencies of linear variable cross-section beams

The geometric configuration of a linear variable cross-section Timoshenko beam is illustrated in Figure. 2. The dimensions of the cross-section varies linearly along the axial direction x.

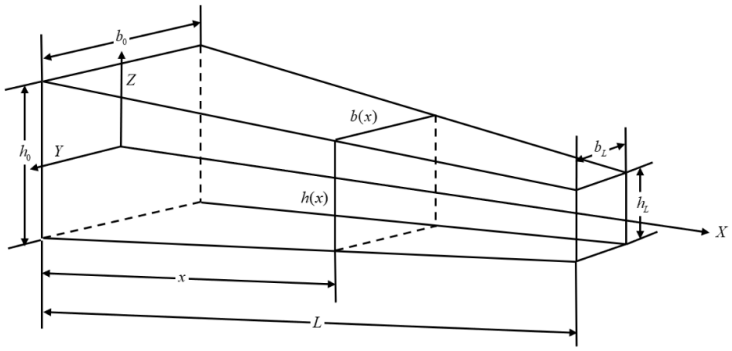


Fig. 2 Schematics of a linear variable cross-section beam

Generally, for linear variable cross-section Timoshenko beams, the height function and width function of a cross section with coordinate x can be represented as:

$$h(x) = h_0 + \frac{h_L - h_0}{L} x \tag{18}$$

$$b(x) = b_0 + \frac{b_L - b_0}{L} x \tag{19}$$

where h_0 and h_L denote the beam height at the left and right side respectfully, b_0 and b_L denote the beam width at the left and right side respectfully . Therefore, the cross-sectional area $A(x)$ and moment of inertia $I(x)$ are:

$$A(x) = b(x)h(x) \tag{20}$$

$$I(x) = \frac{b(x)h(x)^3}{12} \tag{21}$$

Similar to uniform Timoshenko beams, the element strain energy density is expressed as:

$$\begin{aligned} u &= \frac{1}{2} EI(x) \left(\frac{\partial \varphi}{\partial x} \right)^2 + \frac{1}{2} kGA(x) \left(\frac{\partial w}{\partial x} - \varphi \right)^2 \\ &= \frac{1}{2} \boldsymbol{q}^{e\mathrm{T}} \left[EI(x) \boldsymbol{N}_\varphi{}'^{\mathrm{T}} \boldsymbol{N}_\varphi{}' + kGA(x) \left(\boldsymbol{N}_w{}' - \boldsymbol{N}_\varphi \right)^{\mathrm{T}} \left(\boldsymbol{N}_w{}' - \boldsymbol{N}_\varphi \right) \right] \boldsymbol{q}^e \end{aligned} \tag{22}$$

where E is elastic modulus, G is shear modulus, and terms $\frac{\partial \varphi}{\partial x}$ and $\frac{\partial w}{\partial x} - \varphi$ represent the bending curvature and the shear strain, respectively.

The kinetic energy is provided by the inertial contributions caused by transverse translation and cross-sectional rotation, written as:

$$\begin{aligned} T &= \frac{1}{2} \int_0^L \left[\rho A(x) \dot{w}^2 + \frac{1}{2} \rho I(x) \dot{\varphi}^2 \right] dx \\ &= \frac{1}{2} \int_0^L \left[\rho A(x) (\dot{\boldsymbol{q}}^{e\mathrm{T}} \boldsymbol{N}_w{}^{\mathrm{T}} \boldsymbol{N}_w \dot{\boldsymbol{q}}^e) + \frac{1}{2} \rho I(x) (\dot{\boldsymbol{q}}^{e\mathrm{T}} \boldsymbol{N}_\varphi{}^{\mathrm{T}} \boldsymbol{N}_\varphi \dot{\boldsymbol{q}}^e) \right] dx \\ &= \frac{1}{2} \dot{\boldsymbol{q}}^{e\mathrm{T}} \int_0^L \left[\rho A(x) \boldsymbol{N}_w{}^{\mathrm{T}} \boldsymbol{N}_w + \rho I(x) \boldsymbol{N}_\varphi{}^{\mathrm{T}} \boldsymbol{N}_\varphi \right] dx \dot{\boldsymbol{q}}^e \end{aligned} \tag{23}$$

The expressions for the element stiffness $\boldsymbol{K}^e$ and mass matrices $\boldsymbol{M}^e$ are :

$$\boldsymbol{K}^e = \int_0^L [\, EI(x) \boldsymbol{B}_b{}^e \boldsymbol{B}_b + kGA(x) \boldsymbol{B}_s{}^e \boldsymbol{B}_s \,] dx \tag{24}$$

$$\boldsymbol{M}^e = \int_0^L [\rho A(x) \boldsymbol{N}_w{}^{\mathrm{T}} \boldsymbol{N}_w + \rho I(x) \boldsymbol{N}_\varphi{}^{\mathrm{T}} \boldsymbol{N}_\varphi] dx \tag{25}$$

By assembling the element matrices, the global stiffness matrix $\boldsymbol{K}$ and mass matrix $\boldsymbol{M}$ are obtained. The corresponding equation of motion for vibration control is $\left(\boldsymbol{K} - \omega^2 \boldsymbol{M}\right)\boldsymbol{q} = 0$, so the condition for nontrivial solution of the nodal displacements is:

$$\left|\boldsymbol{K} - \omega^2 \boldsymbol{M}\right| = 0 \tag{26}$$

where ω is the natural frequency, which can be obtained by solving the eigenvalue problem.

1.3 Calculation for Timoshenko beams by a conventional FEM

To compare the effect of the present Timoshenko beam element, we provide a conventional FEM without the fusion step of the internal forces in the expression of the displacement field.

For conventional Timoshenko beam element, a cubic polynomial is typically utilized to represent the sum of transverse and shear displacements. Consequently, we have:

$$v = H_1(\xi) v_1 + H_2(\xi) v_1' + H_3(\xi) v_2 + H_4(\xi) v_2' \tag{27}$$

where H_1, H_2, H_3, H_4 are the cubic Hermite interpolation functions, which have the same expressions as Eq. (8). Considering the effect of shear deformation, the rotation at any point within the element is expressed as: $\frac{\partial v}{\partial x} = \gamma + \varphi$, where φ is the cross-sectional rotation, and γ represents the additional rotation angle induced by shear deformation. Then bending deflection in the Timoshenko beam element is obtained as

$$v = H_1(\xi) v_1 + H_2(\xi)(\gamma_1 + \varphi_1) + H_3(\xi) v_2 + H_4(\xi)(\gamma_2 + \varphi_2) \tag{28}$$

The displacement can be expressed as:

$$\begin{aligned} v &= \boldsymbol{N}_v \cdot \bar{\boldsymbol{q}}^e \\ &= \left[H_1(\xi)\ H_2(\xi)\ H_2(\xi)\ H_3(\xi)\ H_4(\xi)\ H_4(\xi)\right] \begin{Bmatrix} v_1 \\ \gamma_1 \\ \varphi_1 \\ v_2 \\ \gamma_2 \\ \varphi_2 \end{Bmatrix} \end{aligned} \tag{29}$$

where $\bar{\boldsymbol{q}}^e$ is a vector including six nodal variables, i.e. $\bar{\boldsymbol{q}}^e = \{v_1\ \gamma_1\ \varphi_1\ v_2\ \gamma_2\ \varphi_2\}^{\mathrm{T}}$, $\boldsymbol{N}_v$ is the shape function for the deflection, and

$\boldsymbol{N}_v = [H_1(\xi)\ \ H_2(\xi)\ \ H_2(\xi)\ \ H_3(\xi)\ \ H_4(\xi)\ \ H_4(\xi)]$.

To achieve high computational accuracy without introducing excessive degrees of freedom, the shear deformation is expressed using a linear function as:

$$\varphi = [N_{\varphi 1}\ \ N_{\varphi 2}][\varphi_1\ \ \varphi_2]^T = (\frac{1-x}{l})\varphi_1 + (\frac{x}{l})\varphi_2 \tag{30}$$

where $N_{\varphi 1}$ and $N_{\varphi 2}$ are the shape functions for the rotation angle with the form of $N_{\varphi 1}=1-\frac{x}{l}, N_{\varphi 2}=\frac{x}{l}$.

The shear deformation can also be written as

$$\varphi = \boldsymbol{N}_\varphi \overline{\boldsymbol{q}}^e \tag{31}$$

where $\boldsymbol{N}_\varphi$ is the shape function matrix for the rotation angle with the following form

$\boldsymbol{N}_\varphi = [0 \quad 0 \quad 1-\frac{x}{l} \quad 0 \quad 0 \quad \frac{x}{l}]$.

Meanwhile, according to the total potential energy functional of the Timoshenko beam element, it can be deduced that:

$$\Pi_e = \frac{1}{2}\overline{\boldsymbol{q}}^{e\mathrm{T}}(\boldsymbol{K}_B^e + \boldsymbol{K}_S^e)\overline{\boldsymbol{q}}^e - \boldsymbol{F}^{e\mathrm{T}}\overline{\boldsymbol{q}}^e \tag{32}$$

where the stiffness matrices $\boldsymbol{K}_B^e$, $\boldsymbol{K}_S^e$ are

$$\begin{cases} \boldsymbol{K}_{\boldsymbol{B}}^{\boldsymbol{e}} = \int_0^1 EI\boldsymbol{B}_{\boldsymbol{b}}^{\boldsymbol{T}}\boldsymbol{B}_{\boldsymbol{b}}dx \\ \boldsymbol{K}_{\boldsymbol{S}}^{\boldsymbol{e}} = \int_0^1 kG\boldsymbol{B}_{\boldsymbol{s}}^{\boldsymbol{T}}\boldsymbol{B}_{\boldsymbol{s}}dx \end{cases} \tag{33}$$

and the strain matrices are

$$\begin{cases} \boldsymbol{B}_b = \dfrac{\partial \boldsymbol{N}_\varphi}{\partial \xi}\cdot\dfrac{1}{L} \\ \boldsymbol{B}_s = \dfrac{\partial \boldsymbol{N}_v}{\partial \xi}\cdot\dfrac{1}{L} - \boldsymbol{N}_\varphi \end{cases} \tag{34}$$

By taking the variation of Eq. (32), the nodal equilibrium equation for the entire structure is obtained as $\boldsymbol{K}^e \cdot \overline{\boldsymbol{q}}^e = \boldsymbol{F}^e$.

For free vibration problem, by assembling the discretized element matrices, the global stiffness $\boldsymbol{K}$ and mass matrices $\boldsymbol{M}$ are obtained. The natural frequencies and the modes of the beam can be similarly obtained by solving the matrix eigenvalue problem as the approach in section 1.2.

1.4 Calculation of the natural frequencies and modes for uniform beams

In the finite element analysis, the stiffness and mass matrices of the proposed beam element can be derived via continuum energy expressions. For Timoshenko beams, kinematic assumptions allow independent transverse displacement and rotation. The

strain energy is contributed by bending deformation and shear deformation respectively. The specific element strain energy density is expressed as:

$$\begin{aligned} u &= \frac{1}{2} EI\left(\frac{\partial \varphi}{\partial x}\right)^2 + \frac{1}{2} kGA\left(\frac{\partial w}{\partial x} - \varphi\right)^2 \\ &= \frac{1}{2}\boldsymbol{q}^{eT}\left[EI\boldsymbol{N}_{\varphi}'^{T}\boldsymbol{N}_{\varphi}' + kGA(\boldsymbol{N}_{w}' - \boldsymbol{N}_{\varphi})^{T}(\boldsymbol{N}_{w}' - \boldsymbol{N}_{\varphi})\right]\boldsymbol{q}^{e} \end{aligned} \tag{35}$$

where EI is the bending stiffness, kGA is the effective shear stiffness.

From Eq. (35), the element stiffness matrix $\boldsymbol{K}^e$ can be obtained as:

$$\boldsymbol{K}^e = \int_0^1 (EI\boldsymbol{B}_b^{\,e}\boldsymbol{B}_b + kGA\boldsymbol{B}_s^{\,e}\boldsymbol{B}_s)Ld\xi \tag{36}$$

The kinetic energy is composed of the inertial contributions caused by transverse translation and cross-sectional rotation, which is written as:

$$\begin{aligned} T &= \frac{1}{2}\int_0^L (\rho A\dot{w}^2 + \rho I\dot{\varphi}^2)dx \\ &= \frac{1}{2}\dot{\boldsymbol{q}}^{e\mathrm{T}}\rho\int_0^L (A\cdot\boldsymbol{N}_w^{\,\mathrm{T}}\boldsymbol{N}_w + I\cdot\boldsymbol{N}_{\varphi}^{\,\mathrm{T}}\boldsymbol{N}_{\varphi})dx\dot{\boldsymbol{q}}^{e} \end{aligned} \tag{37}$$

where the dot denotes differentiation with respect to t. The element mass matrix is obtained as:

$$\boldsymbol{M}^e = \int_0^1 (\rho A\boldsymbol{N}_w^{\,\mathrm{T}}\boldsymbol{N}_w + \rho J\boldsymbol{N}_{\varphi}^{\,\mathrm{T}}\boldsymbol{N}_{\varphi})Ld\xi \tag{38}$$

By assembling the discretized element matrices, the global stiffness $\boldsymbol{K}$ and mass matrices $\boldsymbol{M}$ are obtained. The corresponding equation of motion for the undamped free vibration of the system is: $\boldsymbol{M}\ddot{\boldsymbol{q}} + \boldsymbol{K}\boldsymbol{q} = 0$. To solve for the natural frequencies, the nodal displacement vector $\boldsymbol{q}(t)$ is assumed to be in the harmonic form $q(t) = \phi e^{i\omega t}$, where ϕ denotes the mode shape amplitude vector and ω is the natural frequency. Substituting this harmonic assumption into the equation of motion leads to $\left(\boldsymbol{K} - \omega^2\boldsymbol{M}\right)\boldsymbol{q} = 0$. The condition for the nodal displacements to have a nontrivial solution is:

$$\left|\boldsymbol{K} - \omega^2\boldsymbol{M}\right| = 0 \tag{39}$$

Natural frequencies can be obtained by solving the matrix eigenvalue problem, and the mode shapes can be acquired by the eigenvectors corresponding to the displacement field.

2. Numerical Results

The material parameters for the Timoshenko beam studied in this paper are defined as follows: Young's modulus E=210×10^{9}Pa, Poisson's ratio v=0.3, density $\rho = 7850\text{kg}\cdot\text{m}^{-3}$, and cross-sectional shear coefficient $\mu = \frac{5}{6}$. For uniform beam, the beam length is l=8m, cross-sectional width b=0.25m, the cross-sectional height h=0.5m. The tapered beam will be considered with detailed dimensional data in section 2.1.4.

Three cases of the boundary conditions considered are respectively simply supported at both ends, clamped at both ends, and clamped at one end with the other end free. For ease of discussion, these boundary conditions are denoted as follows: clamped boundaries by "C", free boundaries by "F", and simply-supported boundaries by "S". The beam boundary conditions are labeled along the beam length from left to right; for instance, "C-C" denotes a beam clamped at both ends. These notations will be utilized in subsequent numerical validations and comparative analyses with results from the literature. Furthermore, the first six natural frequencies obtained from the conventional Timoshenko beam element, the proposed Timoshenko beam element, and the reference solutions are compared to analyze their variation trends and highlight the advantages of the new proposed element.

The error of estimation $\varepsilon_\xi = |\xi_{num} - \xi_{ex}|/\xi_{ex}$ for a parameter which can be a displacement component or an internal force component, where ξ_{num} and ξ_{ex} are respectively the numerical value and the exact value. If there is no exact value, the value obtained with enough large number of elements by the finite element commercial software ABAQUS is used.

Table 1. Displacement and force boundary conditions for Timoshenko beams

Boundary condition	Deflection (w)	Cross-sectional angle (φ)	Shear force (Q)	Bending moment (M)
Simple	0	–	–	0
Clamped	0	0	–	–
Free	–	–	0	0

Note**:** The symbol "-" means no restriction of the value.

2.1 Frequency analysis of Timoshenko beam

2.1.1 Free vibration frequency analysis of a simply-supported (S-S) beam

This section analyzes the free vibration characteristics of a Timoshenko beam under simply supported boundary conditions (S-S). To verify the performance of the proposed element, the first six natural frequencies are calculated using both the conventional Timoshenko beam element and the proposed Timoshenko beam element. The results obtained from the proposed element are compared with those from the conventional element and the analytical solutions. Furthermore, to investigate the influence of mesh density on the accuracy of the natural frequencies, the number of elements is chosen as 16, 32 and 48 respectively.

Table 2. The first 6 natural frequencies of S-S Timoshenko beam **(**Unit: rad / s **)**

Number of elements	Element type	Mode number					
		1	2	3	4	5	6
16	The conventional	114.554 (0.159%)	451.544 (0.617%)	992.324 (1.316%)	1709.6 (2.168%)	2571.19 (3.061%)	3543.14 (3.880%)
	The proposed	114.373 (0.001%)	448.882 (0.023%)	980.467 (0.105%)	1678.110 (0.286%)	2509.421 (0.585%)	3445.000 (1.002%)
32	The conventional	114.553 (0.158%)	451.537 (0.615%)	992.247 (1.308%)	1709.17 (2.142%)	2569.6 (2.997%)	3538.41 (3.741%)
	The proposed	114.373 (0.001%)	448.882 (0.023%)	980.461 (0.105%)	1678.07 (0.283%)	2509.29 (0.580%)	3444.61 (0.991%)
48	The conventional	114.553 (0.158%)	451.537 (0.615%)	992.243 (1.307%)	1709.15 (2.141%)	2569.51 (2.994%)	3538.17 (3.734%)
	The proposed	114.373 (0.001%)	448.882 (0.023%)	980.460 (0.104%)	1678.07 (0.283%)	2509.28 (0.580%)	3444.6 (0.991%)
The analytical		114.372	448.777	979.437	1673.328	2494.818	3410.807

Note: The values in parentheses represent the relative errors of the calculated results compared to the analytical solutions.

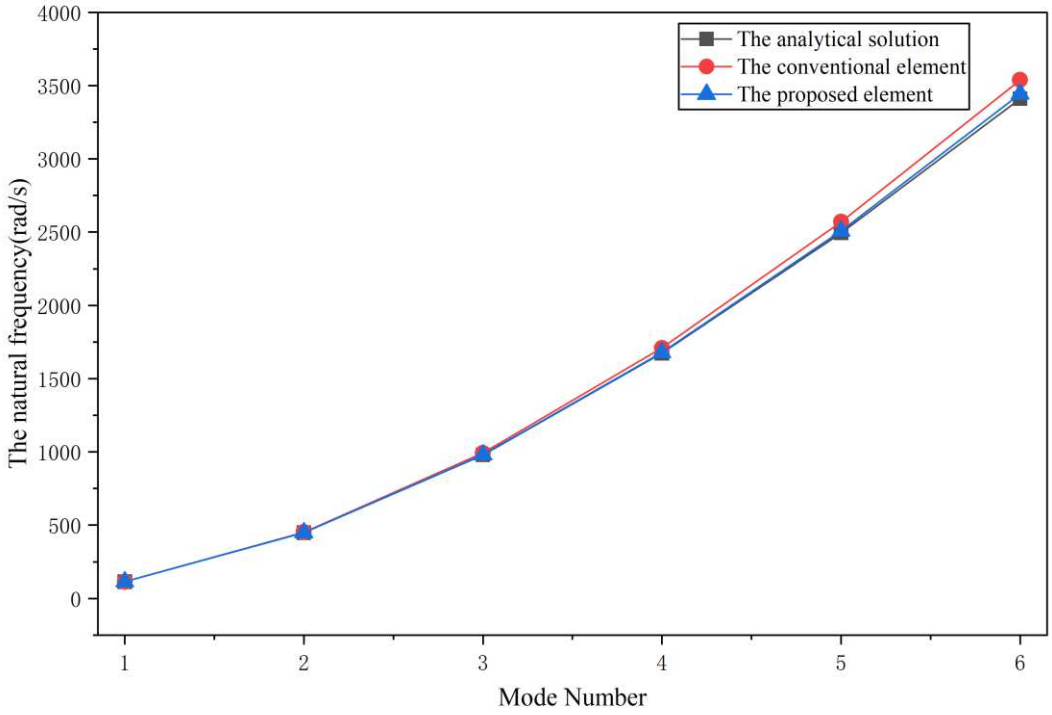


Fig. 3 Comparison of natural frequencies for a simply-supported Timoshenko beam among the three results: the conventional element, the proposed element and the analytical solution (48 elements)

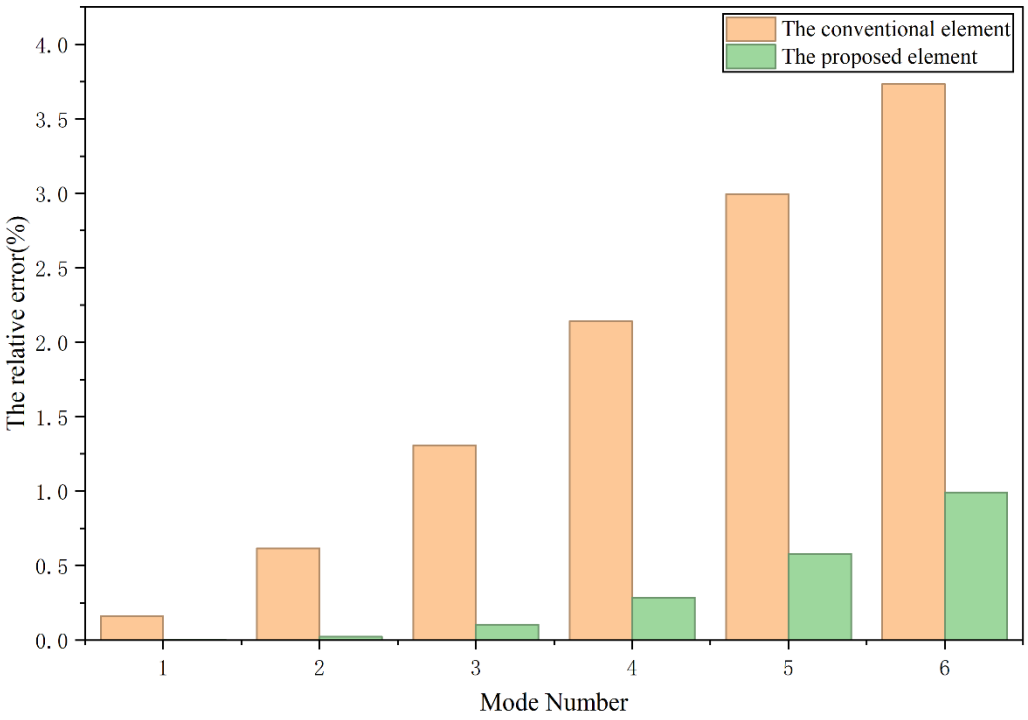


Fig. 4 Comparison of relative errors in natural frequencies for a simply-supported Timoshenko beam (48 elements)

Table 2 reports the first six natural frequencies of S-S Timoshenko beam calculated by the conventional and proposed beam elements under different numbers of elements (16, 32 and 48), in comparison with the exact analytical solutions. The values in parentheses denote the relative errors relative to the analytical solutions. Figure 1 presents the comparison of the first six natural frequencies for the simply-supported Timoshenko beam obtained using the conventional beam element, the proposed beam element, and the exact analytical solutions. To visually evaluate the computational accuracy, Figure 4 depicts the corresponding relative errors of the obtained frequencies by two beam elements under a discretization of 48 elements from mode 1 to mode 6, where the orange and green bars denote the relative errors of the conventional and proposed beam elements with respect to the analytical solutions, respectively.

From Figure 4, the natural frequencies obtained from the various elements are highly consistent at lower modes. As the mode order increases, the difference in the calculated results between the proposed element and the conventional becomes progressively pronounced. Concurrently, a comparison of the first six natural frequencies under different numbers of elements with the analytical solutions in Table 4 reveals that the computational accuracy of the proposed beam element is remarkably superior to that of the conventional Timoshenko beam element.

It can be concluded from Figure 3 that even with a relatively small number of elements, the relative error of the proposed element compared to the analytical solution is strictly confined to within 1%. In contrast, the error of the conventional element predominantly exceeds 2%, which is about twice that of the present element. Subsequently, with an increasing number of elements, although the results of both

elements converge to the analytical solutions, the proposed element still maintains a substantially more conspicuous accuracy advantage over the conventional element even for high-order frequencies.

2.1.2 Free vibration frequency analysis of a clamped-clamped (C-C) beam

This section analyzes the free vibration characteristics of a Timoshenko beam under clamped-clamped (C-C) boundary conditions. To verify the performance of the proposed element, the first six natural frequencies are calculated using both the conventional Timoshenko beam element, i.e., in section 1.3, and the present Timoshenko beam element. The results obtained by the proposed element are compared with those by the conventional element and the FEM simulated values by ABAQUS. Furthermore, to investigate the influence of mesh density on the accuracy of the natural frequencies, the number of elements varies as 16, 32 and 48.

Table 3. The first 6 natural frequencies of the C-C Timoshenko beam **(**Unit: rad/s **)**

Number of elements	Element type	Mode number					
		1	2	3	4	5	6
16	The conventional	254.651 (0.177%)	682.534 (0.937%)	1292.52 (1.845%)	2051.56 (2.768%)	2928.46 (3.571%)	3892.77 (4.152%)
	The proposed	254.19 (-0.004%)	678.335 (0.316%)	1277.72 (0.679%)	2017.46 (1.060%)	2868.2 (1.439%)	3805.11 (1.806%)
32	The conventional	254.65 (0.177%)	682.51 (0.933%)	1292.35 (1.832%)	2050.82 (2.731%)	2926.08 (3.486%)	3886.46 (3.983%)
	The proposed	254.19 (-0.004%)	678.333 (0.315%)	1277.7 (0.678%)	2017.4 (1.057%)	2868 (1.432%)	3804.59 (1.792%)
48	The conventional	254.65 (0.177%)	682.508 (0.933%)	1292.34 (1.831%)	2050.78 (2.729%)	2925.96 (3.482%)	3886.14 (3.974%)
	The proposed	254.19 (-0.004%)	678.333 (0.315%)	1277.7 (0.678%)	2017.4 (1.057%)	2867.99 (1.432%)	3804.58 (1.792%)
FEM by ABAQUS		254.2	676.2	1269.1	1996.3	2827.5	3737.6

Note: The values in parentheses represent the relative errors of the calculated results compared to the analytical solutions.

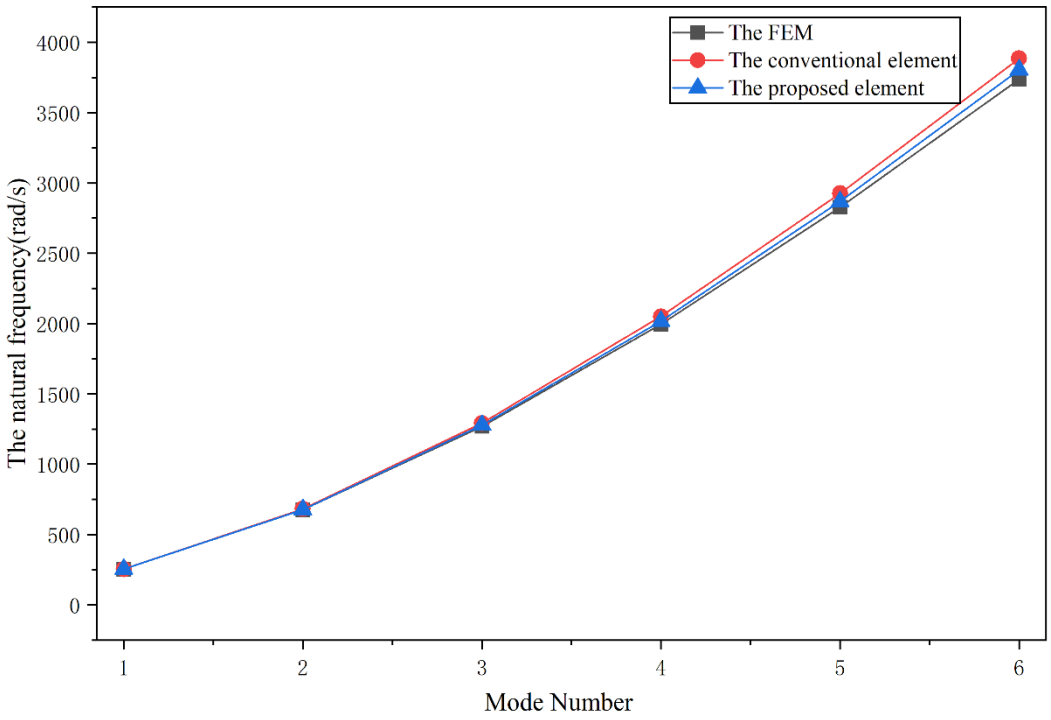


Fig. 5 Comparison of natural frequencies for a C-C Timoshenko beam among the three results: the conventional element, the proposed element and the FEM (48 elements)

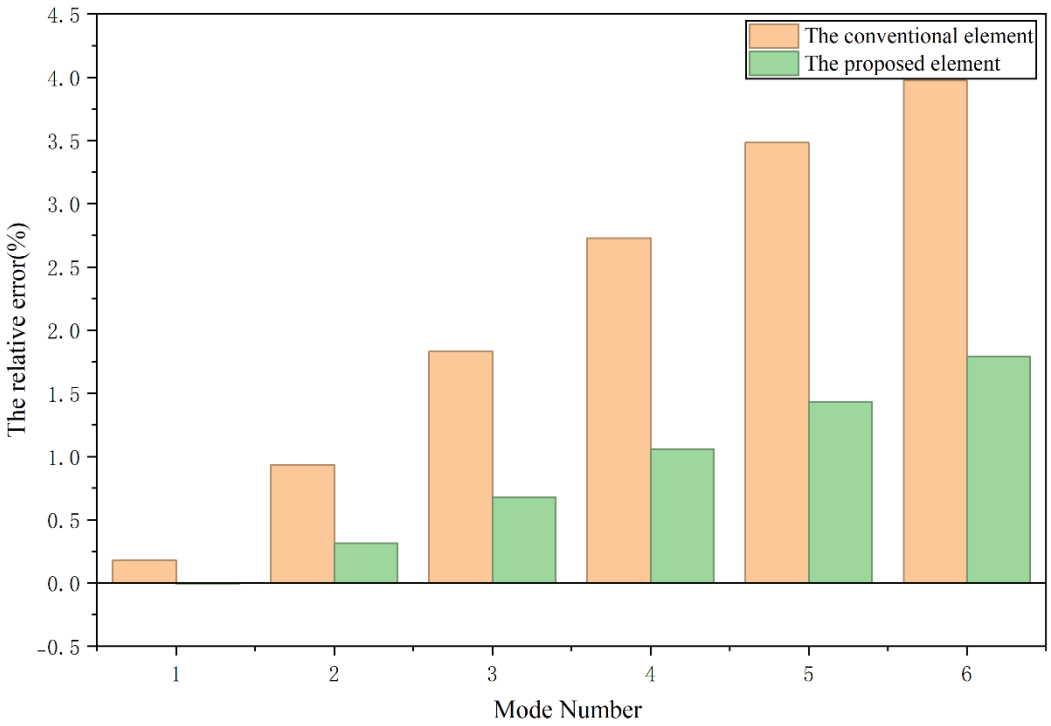


Fig. 6 Comparison of the relative errors of the natural frequencies for a clamped-clamped Timoshenko beam (48 elements)

Table 3 presents the first six natural frequencies of the C-C Timoshenko beam calculated by the conventional and proposed beam elements under different numbers

of elements (16, 32 and 48), in comparison with the exact analytical solutions. The values in parentheses denote the relative errors with respect to the analytical solutions. Figure 5 presents the comparison of the first six natural frequencies for the clamped-clamped Timoshenko beam obtained using the conventional beam element, the proposed beam element, and the exact analytical solutions. To evaluate the computational accuracy, Figure 6 depicts the corresponding relative errors of the two kinds of beam elements under a discretization of 48 elements for the first six modes.

From Table 3, the calculated natural frequencies of the conventional Timoshenko beam element at lower modes show a relatively small error of approximately 1% against the ABAQUS simulated values. As the mode order increases, the relative error corresponding to the conventional element progressively escalates, universally exceeding 4% at the sixth mode regardless of the increase in the number of elements.

The relative errors of the proposed element are obtained in Fig. 6. It can be found that for the fundamental frequency, the relative error between the present value by the proposed Timoshenko beam element and the simulated FEM value is negligible. Although the error increases with the mode order, it is noteworthy that the relative error of the novel Timoshenko beam element is merely around 1.8% even at the sixth mode. Furthermore, the relative errors change little for different meshed segments from Table 3. In comparison with the conventional Timoshenko beam element, it is manifest that the error of the traditional beam element is more than twice that of the novel element.

2.1.3 Free vibration analysis of a C-F beam

This section analyzes the free vibration characteristics of a Timoshenko beam under clamped-free (C-F) boundary conditions. To verify the performance of the proposed element, the first six natural frequencies are calculated by using both the conventional Timoshenko beam element (shown in section 1.3) and the proposed beam element under the C-F boundary condition. The results obtained from the proposed Timoshenko beam element are then compared with those from the conventional Timoshenko beam element as well as the simulated values. Furthermore, to investigate whether the number of elements exerts an influence on the accuracy of the natural frequencies, the beam is discretized into 16, 32 and 48 elements respectively.

Table 4. The first 6 natural frequencies of the C-F Timoshenko beam **(**Unit: rad/s **)**

Number of elements	Element type	Mode number					
		1	2	3	4	5	6
16	The conventional	40.917 (-0.202%)	252.893 (0.394%)	692.993 (1.285%)	1317.78 (2.344%)	2099.69 (3.413%)	3006 (4.346%)
	The proposed	40.886 (-0.278%)	251.625 (-0.109%)	685.397 (0.175%)	1294.10 (0.505%)	2048.09 (0.871%)	2916.64 (1.244%)
32	The conventional	40.917 (-0.202%)	252.892 (0.394%)	692.967 (1.281%)	1317.59 (2.329%)	2098.82 (3.370%)	3003.13 (4.246%)

	The proposed	40.886 (-0.278%)	251.625 (-0.109%)	685.395 (0.175%)	1294.09 (0.504%)	2048.02 (0.868%)	2916.42 (1.236%)
48	The conventional	40.917 (-0.202%)	252.892 (0.394%)	692.925 (1.275%)	1317.58 (2.328%)	2098.78 (3.368%)	3002.98 (4.241%)
	The proposed	40.886 (-0.278%)	251.625 (-0.109%)	685.395 (0.175%)	1294.09 (0.504%)	2048.02 (0.868%)	2916.42 (1.236%)
FEM by ABAQUS		41.0	251.9	684.2	1287.6	2030.4	2880.8

Note: The values in parentheses represent the relative errors of the calculated results compared to the analytical solutions.

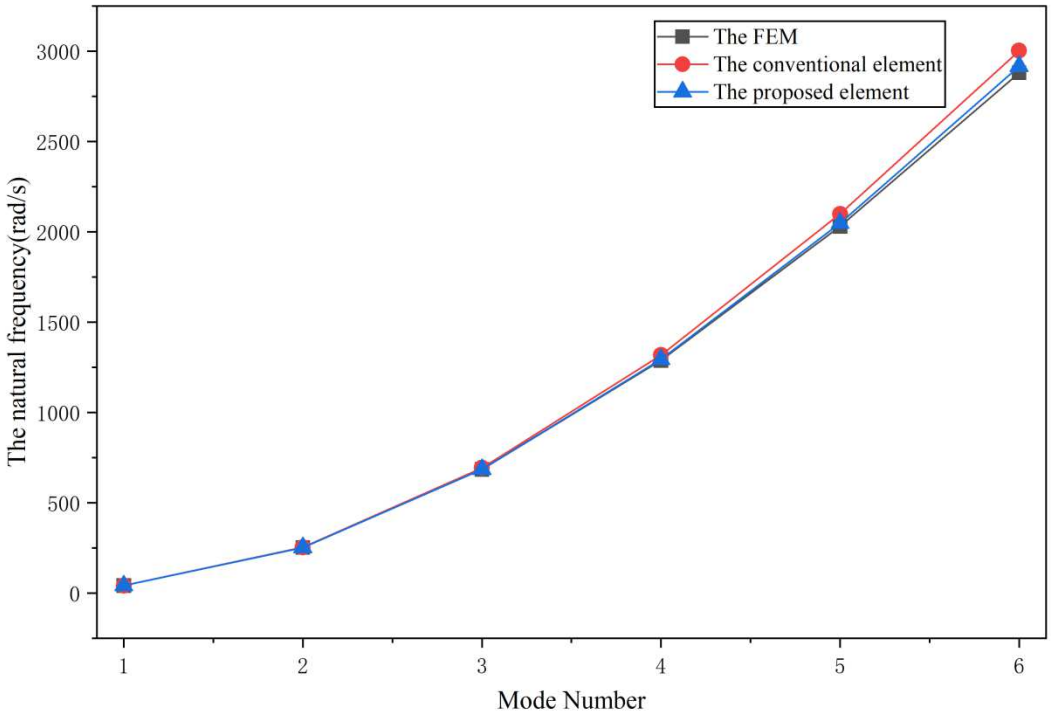


Fig. 7 Comparison of the natural frequencies for a C-F Timoshenko beam among the three results: the conventional element, the proposed element and the FEM (48 elements)

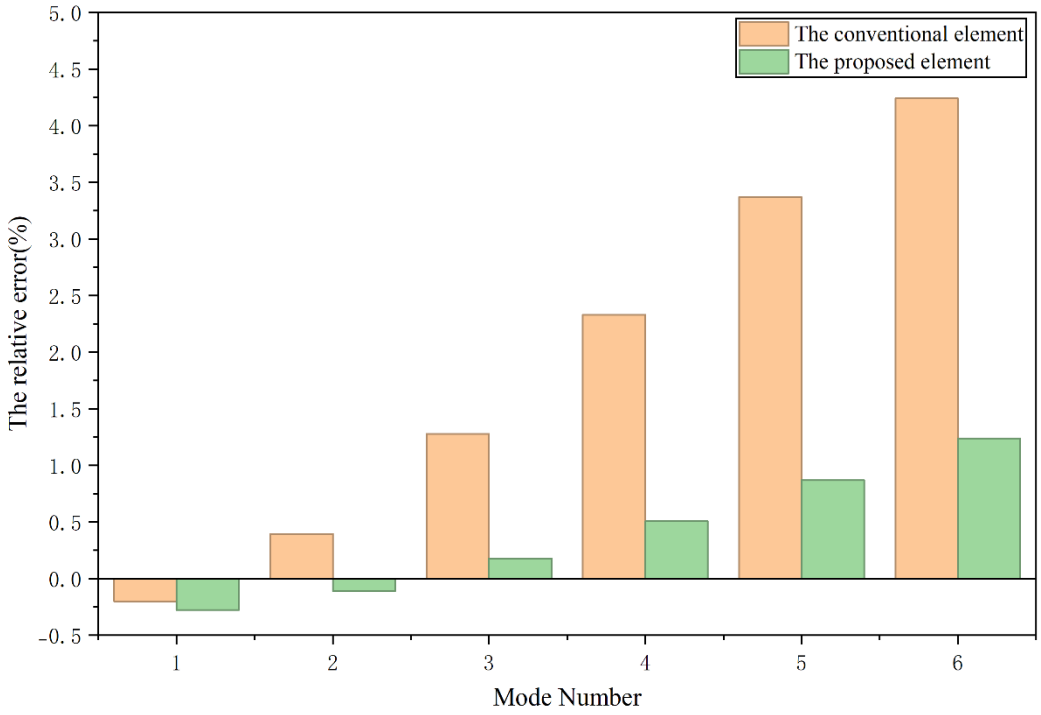


Fig. 8 Comparison of relative errors in natural frequencies for a C-F Timoshenko beam (48 elements)

Table 4 reports the first six natural frequencies of the C-F Timoshenko beam calculated by the conventional and the proposed beam elements under different numbers of elements (16, 32 and 48) in comparison with the exact analytical solutions. The values in parentheses denote the relative errors with respect to the analytical solutions. Figure 7 presents the comparison of the first six natural frequencies for the C-F Timoshenko beam obtained using the conventional beam element, the proposed beam element, and the exact analytical solutions. To evaluate the computational accuracy, Figure 8 depicts the corresponding relative errors of the first 6 frequencies by the present and conventional elements under a discretization of 48 elements.

It can be concluded from Figure 8 that for lower modes, the calculated natural frequencies by the conventional Timoshenko beam element show a relatively small error of approximately 1% against the ABAQUS simulated values, consistent with the trends from of the cases of the S-S and C-C beams in Fig. 3 and Fig. 5. Nevertheless, as the mode order increases the relative error progressively get larger for the conventional element, universally exceeding 4% at the sixth mode for all the three cases of the elements number. Meanwhile, for the present Timoshenko beam element the corresponding relative errors are much less than that of the conventional one, even for the case of 16-element-division from Table 4. For the fundamental frequency, the absolute value of relative error between the obtained natural frequency and the simulated FEM value by ABAQUS is less than 0.3%. Although the error increases with the mode order, it is noteworthy that the relative error of the proposed element is merely around 1.236% even at the sixth mode. In comparison with the conventional Timoshenko beam element, it is manifest that most of the relative errors by the proposed

beam element is just one third or less of that of the conventional element. Furthermore, the discrepancy between the conventional element and the proposed element in error of the obtained natural frequency gradually expands with the increasing mode order. These demonstrate the stability and the efficiency of the proposed Timoshenko beam element.

2.1.4 Frequency analysis of a linear variable cross-section Timoshenko beam

This section analyzes the free vibration characteristics of a linear variable cross-section Timoshenko beam under clamped-free boundary condition (C-F).

As shown in Fig. 2, the beam length is $l = 10h_0$, h_0=b_0=0.8m, the taper ratios are defined as $\beta_b = 1 - b_L / b_0, \beta_h = 1 - h_L / h_0$. Here β_b and β_h are selected equally as 0.1, 0.5 or 0.9. To thoroughly verify the performance and capability of the proposed element, the first six natural frequencies of the Timoshenko beam under the C-F boundary condition are calculated. The results obtained by the proposed element are compared with the simulated values available in the literature. Furthermore, to investigate whether the number of elements exerts an influence on the accuracy of the natural frequencies, the beam is discretized into 16, 32 and 48 elements, respectively. The natural frequencies are non-dimensionalized by $\lambda = \omega \cdot L^2 \sqrt{\frac{\rho \cdot A(L)}{E \cdot I(L)}}$.

Table 5 presents the first five non-dimensional natural frequencies of the linear-variable-cross-section C-F Timoshenko beam calculated by the proposed beam element under different taper ratios (0.1, 0.5, and 0.9) and numbers of elements (16, 32 and 48), in comparison with the FEM solutions by ABAQUS. The values in parentheses denote the relative errors with respect to the analytical solutions. To evaluate the computational accuracy, Figure 9 depicts the corresponding relative errors of the first five natural frequencies by using 48 discrete proposed elements.

Table 5. The first 5 non-dimensional natural frequencies of the C-F Timoshenko beam with linear variable cross-section

Taper Ratio	Element Type	Number of element	Mode number				
			1	2	3	4	5
0.1	The proposed	16	3.64619 (0.00%)	20.5661 (-0.04%)	53.3817 (-0.10%)	97.0037 (-0.61%)	148.287 (-0.23%)
		32	3.6461 (-0.01%)	20.5658 (-0.04%)	53.3808 (-0.10%)	97.0018 (-0.61%)	148.283 (-0.23%)
		48	3.6461 (-0.01%)	20.5657 (-0.04%)	53.3807 (-0.10%)	97.0015 (-0.61%)	148.282 (-0.23%)
	FEM by ABAQUS		3.6463	20.5748	53.4334	97.6014	148.6233
0.5	The proposed	16	4.5956 (0.07%)	18.9666 (0.07%)	45.4007 (0.03%)	81.7726 (-0.03%)	125.988 (-0.10%)
		32	4.5929 (0.02%)	18.9524 (-0.01%)	45.3659 (-0.05%)	81.7127 (-0.11%)	125.901 (-0.17%)
		48	4.5924	18.9496	45.359	81.7006	125.884

			(0.00%)	(-0.02%)	(-0.06%)	(-0.12%)	(-0.19%)
	FEM by ABAQUS		4.5922	18.9535	45.3884	81.8008	126.118
0.9	The proposed	16	7.1803 (0.46%)	18.5369 (1.07%)	36.3814 (1.44%)	60.9928 (1.57%)	91.8935 (1.58%)
		32	7.1559 (0.12%)	18.3932 (0.29%)	36.0014 (0.38%)	60.2856 (0.40%)	90.79 (0.36%)
		48	7.1511 (0.05%)	18.3632 (0.12%)	35.919 (0.15%)	60.1309 (0.14%)	90.549 (0.09%)
	FEM by ABAQUS		7.1472	18.3404	35.8636	60.0477	90.4673

Note: The values in parentheses represent the relative errors of the calculated results compared to the analytical solutions.

From low-order-mode results in Table 5, the present calculated natural frequencies of the variable cross-section Timoshenko beam are consistent with the FEM simulated values. However, as the mode order increases, the difference in the results between the two beam elements becomes progressively pronounced.

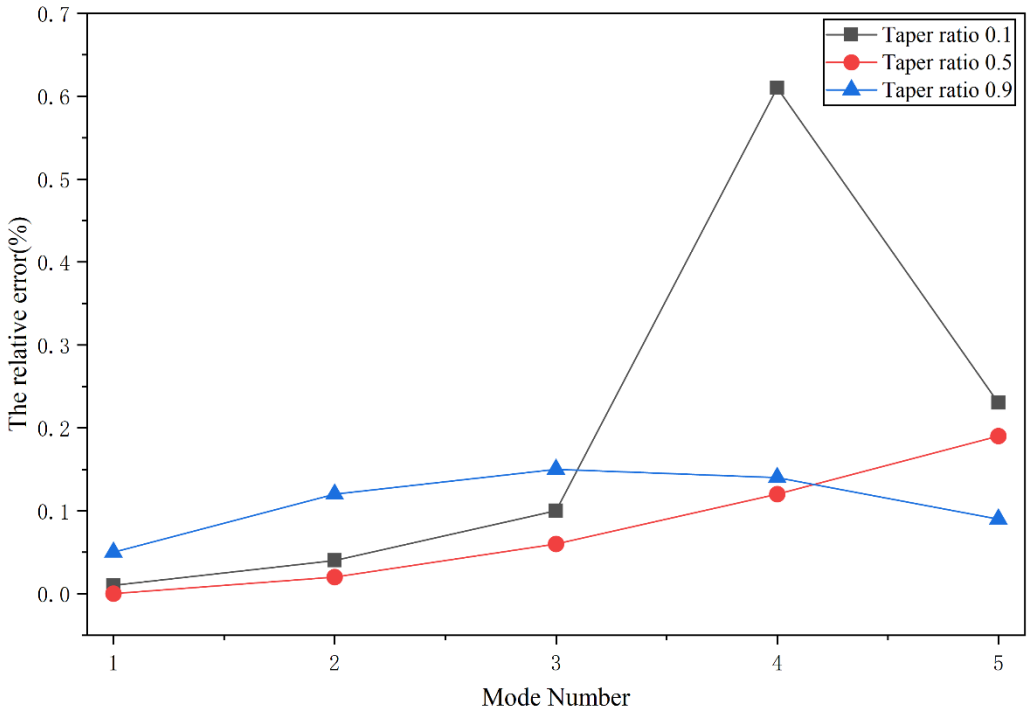


Fig. 9 Errors of the natural frequency by the proposed Timoshenko beam with a linearly variable cross-section under C-F boundary condition (48 elements)

It can be found from Figure 9 that for different mode orders and taper ratios, all the relative errors between the calculated natural frequencies of the proposed element and the ABAQUS results consistently keep well below 1%. As the mode order increases, the relative error progressively improved a little. Specially, for the fundamental frequency, the relative error between the natural frequency of the present beam element

and the FEM results is less than 0.05% for all three cases of the taper ratio. Here the number of elements used is 48. It is noteworthy that the relative error of the present Timoshenko beam element is merely less than 0.2% even at the fifth mode. It's found that the results are good for cases of small values of taper which is affected little by the number of elements divided in Table 5, for example, mesh with 16 elements is enough to generate results with relative errors of the first 5 frequencies less than 0.23% when β_b and β_h are equally as 0.1 or 0.5. When the beam cross section changes sharply, more elements are required to obtain a better precision. For case of β_b=β_h = 0.9, the relative error of the first six natural frequencies is less than 0.4% when 32 elements are divided, and the error decrease to less than 0.15% when 48 divided elements are used. This numerical results demonstrat the excellent precision of the proposed fusion beam element.

2.2 Modal analysis of a uniform simply-supported beam

This section performs a numerical solution of the vibration equations for a uniform Timoshenko beam under simply-supported boundary conditions. The first four natural mode shapes obtained from the proposed element, along with their associated internal force distributions, are systematically compared with the analytical profiles derived from Timoshenko beam theory. Furthermore, to investigate whether the element mesh density exerts an influence on the profiles of these mode shapes and internal force distributions, the beam is discretized into 16, 32 and 48 elements, respectively.

2.2.1 Deflection mode shape

For a simply-supported beam under different mesh refinement levels, Figures 10 to Figure 12 present the comparison between the numerical results and the analytical solutions for the first four deflection mode shapes. In each figure, the horizontal axis represents the coordinate along the beam length, while the vertical axis denotes the normalized deflection amplitude. The four subplots sequentially correspond to the 1st to 4th mode shape. Specifically, Figure 10, 11 and 12 illustrate the obtained mode shapes by using 16, 32 and 48 elements respectively.

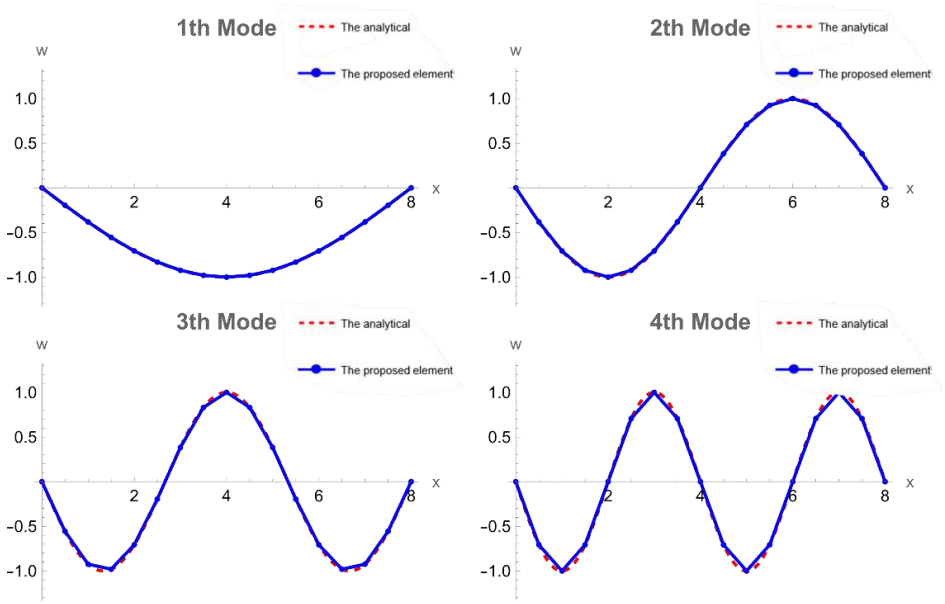


Fig. 10 The first four deflection mode shapes of a simply-supported beam (using 16 elements)

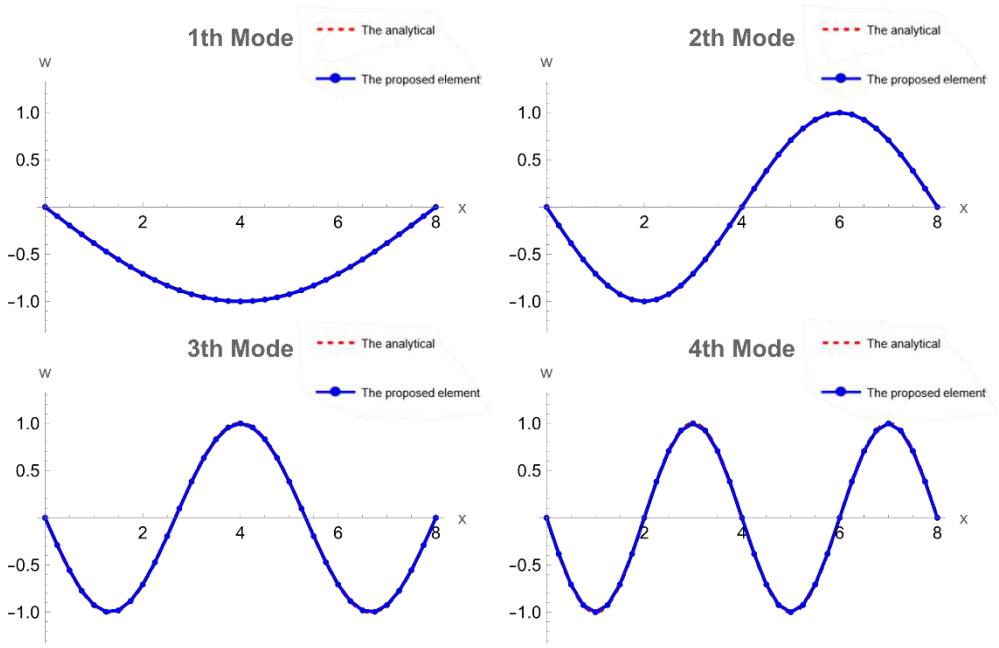


Fig. 11 The first four deflection mode shapes of a simply-supported beam (using 32 elements)

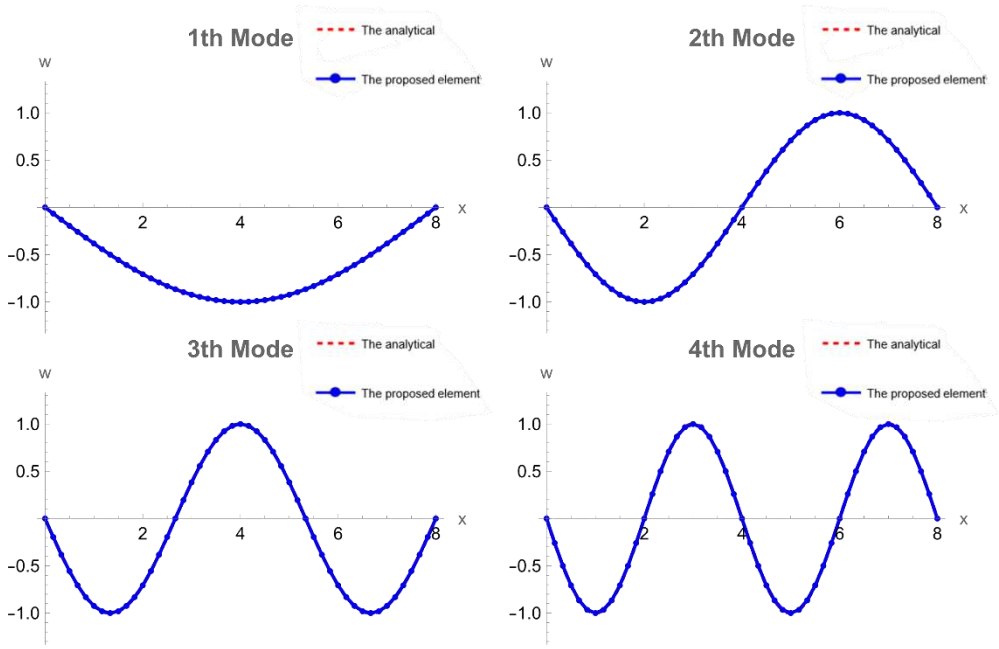


Fig. 12 The first four deflection mode shapes of a simply-supported beam (using 48 elements)

It's known that deflection serves as the most intuitive manifestation of structural vibration. From the first to the fourth modes in Figure 12, it can be clearly observed that the finite element nodes fall accurately on the spatial envelope of the analytical mode shapes. Even under the fourth-order higher mode, the FEM discrete points still seamlessly overlap with the analytical curves, owing to the high accuracy of the proposed novel element. Meanwhile, as the number of elements increases from 16 to 48 the corresponding mode shapes of deflection is shown in Figure 10 to Figure 12, it is apparent that the difference in mode shapes obtained between 16 and 48 elements is negligible. The mode shapes captured by using 48 elements closely approximate the pure harmonic waves corresponding to the analytical modes. Thus it can be concluded that the proposed element leads to good accuracy for the nodal defection.

2.2.2 Rotation mode shape

For a simply-supported beam, Figs. 13 to 15 report the comparison between the numerical results and the analytical solutions for the first four rotation mode shapes under different mesh refinement levels. In each figure, the horizontal axis represents the coordinate along the beam length, while the vertical axis denotes the normalized rotation amplitude. The four subplots sequentially correspond to the 1st to 4th mode shape. Specifically, the number of elements used in Figures 13, 14, and 15 are 16, 32 and 48 respectively.

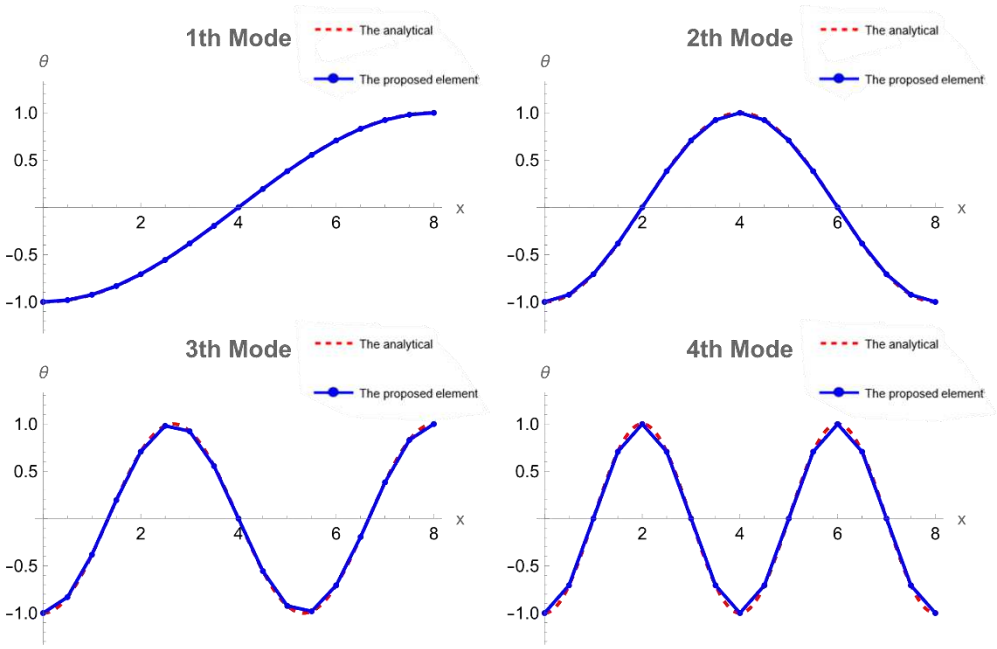


Fig. 13 The first four rotation mode shapes of a simply-supported beam (using 16 elements)

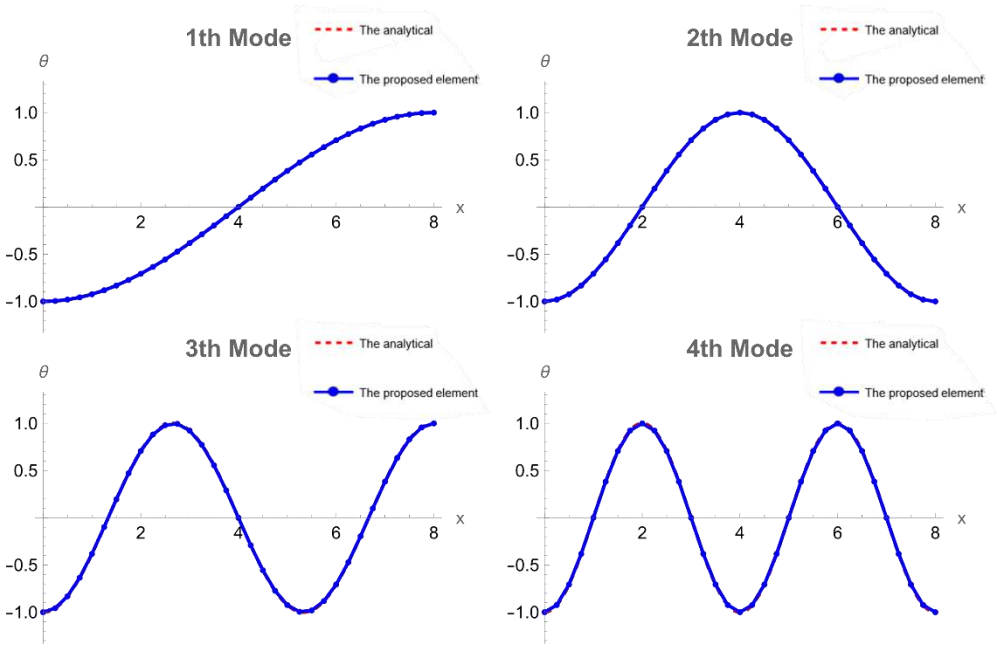


Fig. 14 The first four rotation mode shapes of a simply-supported beam (using 32 elements)

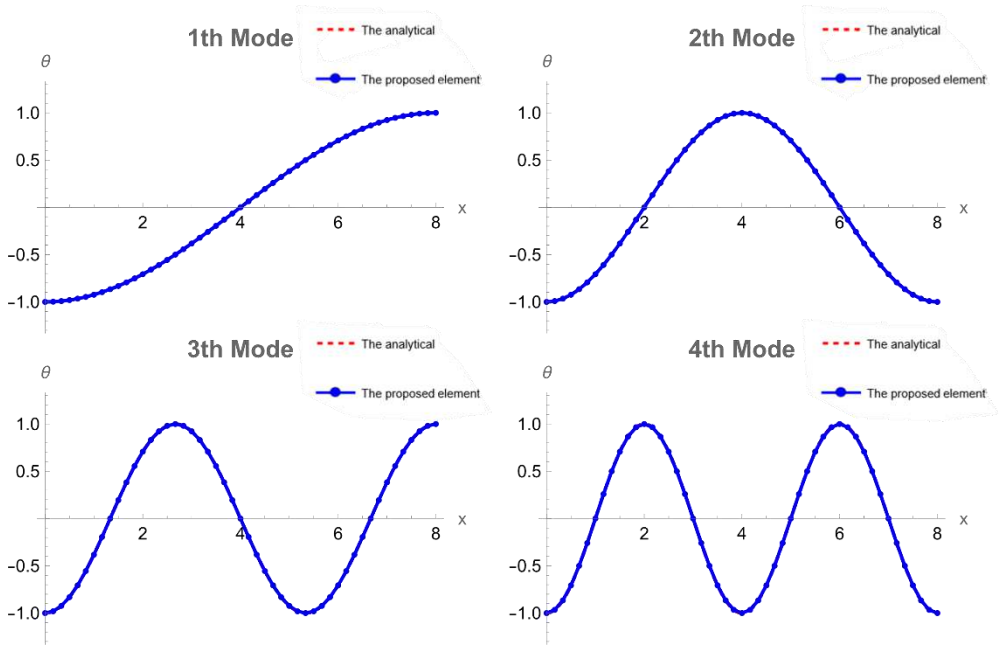


Fig. 15 The first four rotation mode shapes of a simply-supported beam (using 48 elements)

The rotation mode shape reflects the rotational characteristics of the beam cross-section around the neutral axis during vibration. From the first mode to fourth mode, it can be clearly observed from the figure that the nodal rotation values extracted from the present finite element results fall accurately on the spatial envelope of the analytical mode shapes. Even under the fourth-order mode, the discrete points of the present FEM results still seamlessly overlap with the analytical curves, owing to the extremely high computational accuracy of the proposed element in handling rotational degrees of freedom. Meanwhile, comparison of the increasing number of elements from 16 to 48 reveals that the rotation mode shapes obtained with 16 elements are effective in roughly capturing the wave profiles. In contrast, the mode shape profiles yielded by 48 elements closely approximate standard cosine harmonics, thus converging toward the analytical modes. This strongly demonstrates that the proposed element can precisely capture the physical characteristics of rotation extrema at the supports and zero-rotation points at the mid-span when describing cross-sectional rotational behavior.

2.2.3 Shear force distribution

Fig. 16 to Fig. 18 present the comparison between the numerical results and the analytical solutions for the first four shear force distributions of a simply-supported beam under different mesh refinement levels. The number of the proposed element used are 16, 32 and 48 respectively in Figure 16, 17 and 18. In each figure, the horizontal axis represents the coordinate along the beam length, while the vertical axis denotes the normalized shear force amplitude. The four subplots sequentially correspond to the 1st to 4th mode shapes.

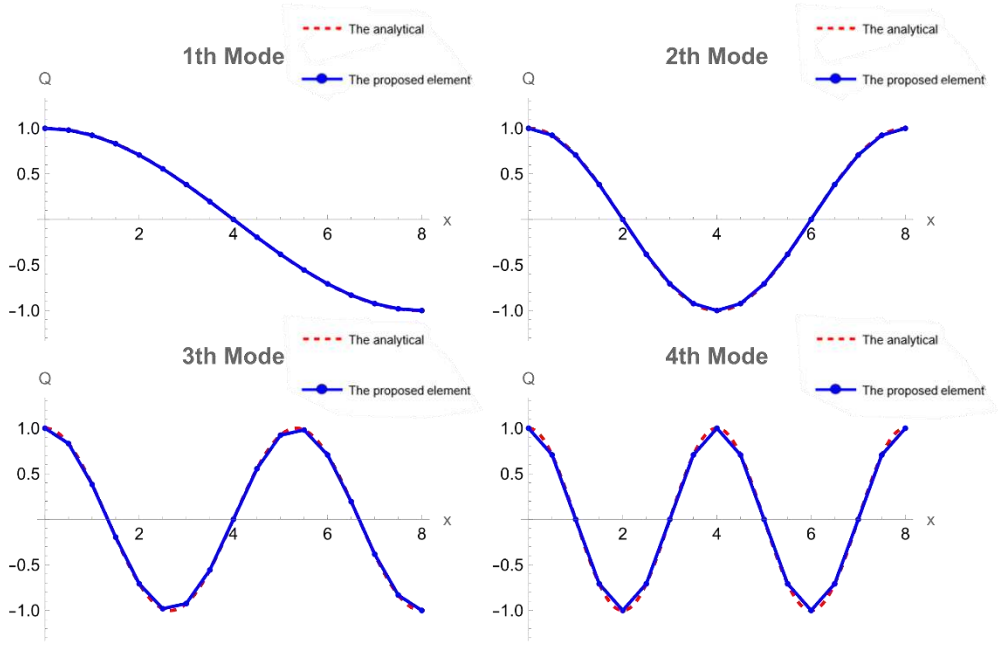


Fig. 16 The first four shear force distributions of a simply-supported beam (using 16 elements)

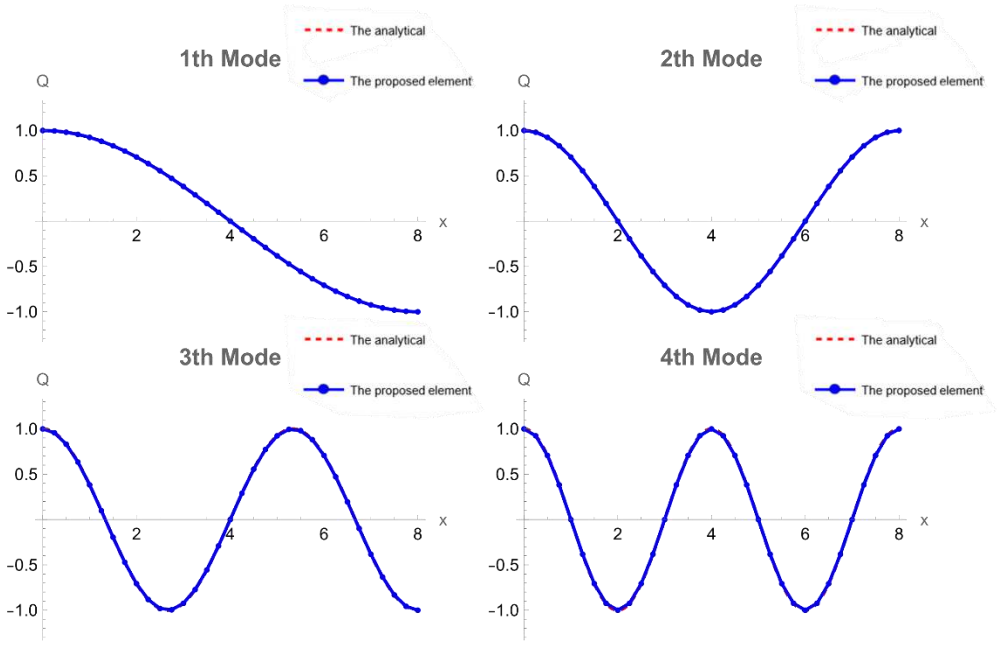


Fig. 17 The first four shear force distributions of a simply-supported beam (using 32 elements)

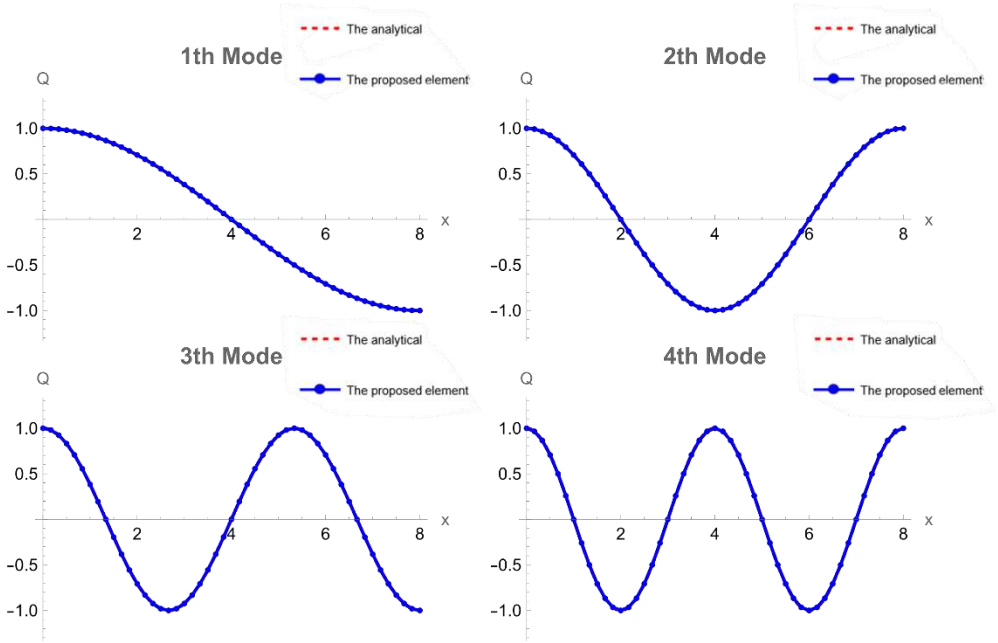


Fig. 18 The first four shear force distributions of a simply-supported beam (using 48 elements)

The shear force distribution reflects the variations of transverse shear force within the internal structure, in which the analytical form can be determined by the shear constitutive relation, i. e., Eq. (4). From the obtained shear force for all the first four modes in Fig. 18, it can be obtained that the values at the nodes by the proposed finite element fall accurately on the spatial envelope of the analytical solutions. Even for the higher mode as the fourth order, the proposed FEM discrete nodal results still seamlessly overlap with the analytical curves, owing to the exceptional accuracy of the proposed novel element in describing shear deformations. Concurrently, a comparison of the increasing number of elements from 16 to 48 reveals that 16 elements are already capable of well capturing the shear force extrema at the boundaries. As the element number increases to 48, the predicted distribution profiles closely approximate pure harmonic waves, thereby highly converging toward the analytical distribution profiles. This demonstrates that when handling dynamic characteristics, the proposed element can precisely maintain the amplitude features of the shear force at the supports and ensure the phase accuracy at internal nodes, fully validating its reliability in structural dynamic analysis.

2.2.4 Bending moment distributions

For a simply-supported beam under different mesh refinement levels, Fig. 19 to Fig. 21 report the comparison between the numerical results and the analytical solutions for the first four bending moment distributions. In each figure, the horizontal axis represents the coordinate along the beam length, while the vertical axis denotes the

normalized bending moment amplitude. The four subplots sequentially correspond to the 1st to 4th mode shapes. The red dashed line represents the analytical solution, and the blue solid line with nodes denotes the finite element results obtained by the proposed element. Specifically, Fig. 19, 20, and 21 illustrate the distributions obtained by using 16, 32 and 48 elements, respectively.

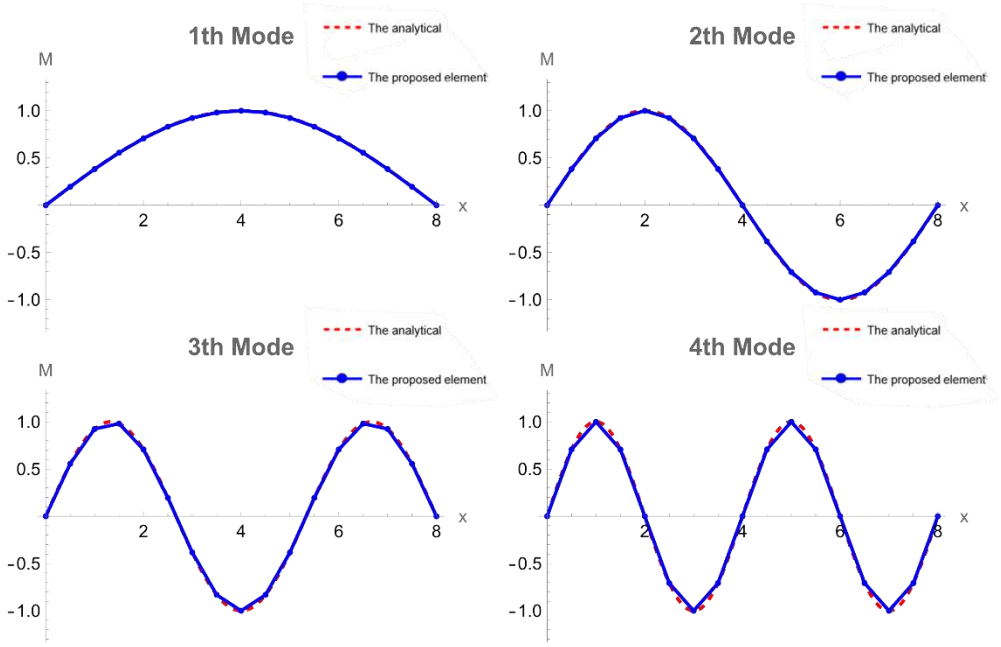


Fig. 19 The first four bending moment distributions of a simply-supported beam (using 16 elements)

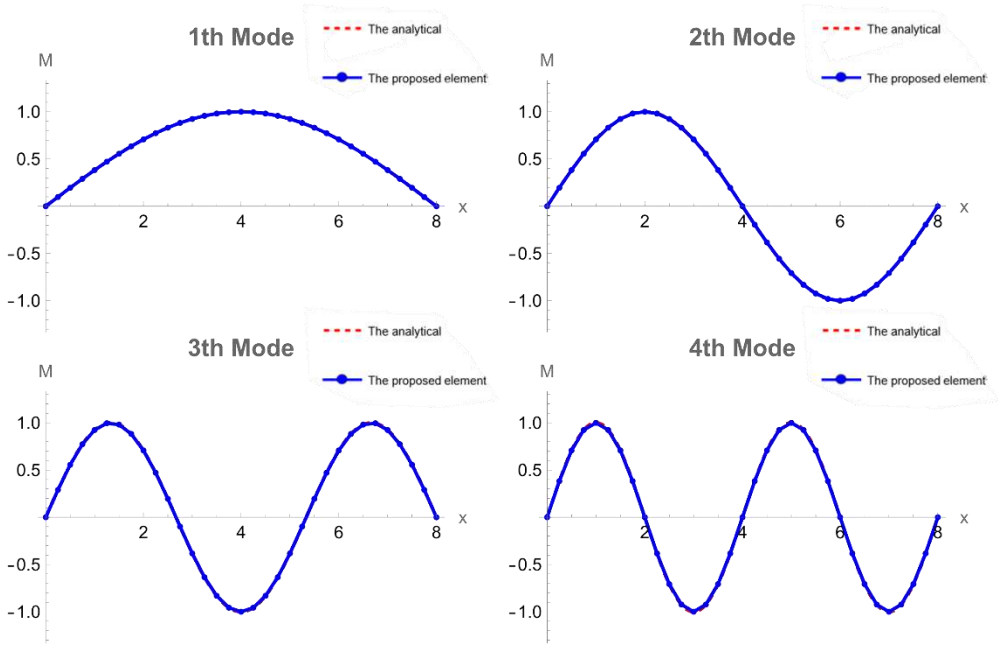


Fig. 20 The first four bending moment distributions of a simply-supported beam (using 32 elements)

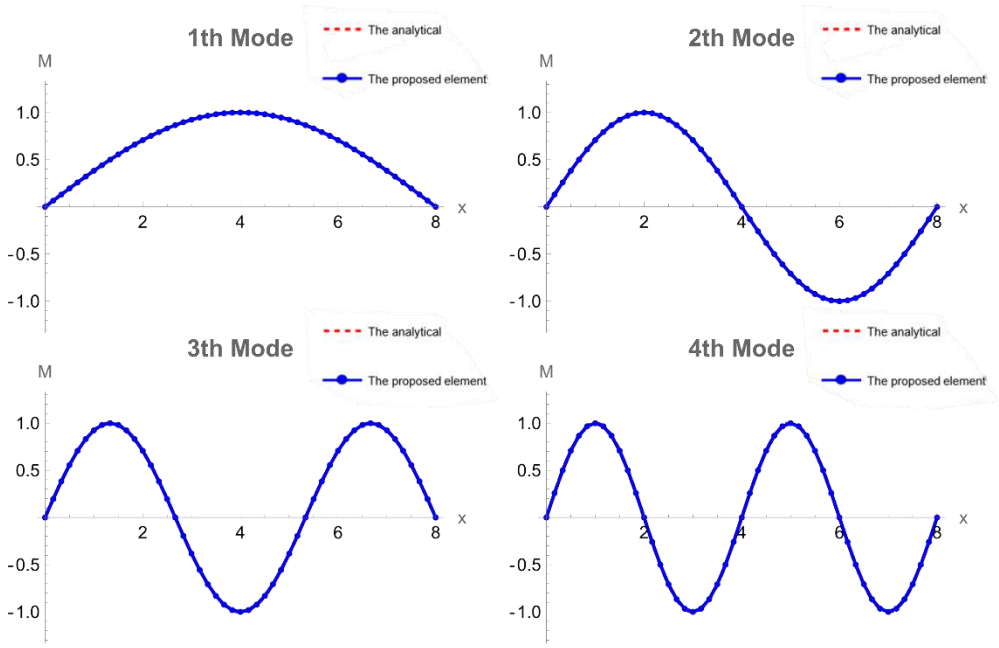


Fig. 21 The first four bending moment distributions of a simply-supported beam (using 48 elements)

The bending moment distribution characterizes the evolution of internal bending moments within the beam during vibration, in which the analytical form of bending

moment is determined by the moment-curvature relationship, i. e., Eq. (3). In numerical computation, the nodal bending moment can be extracted from the eigenvectors in analysis of the proposed element.

From the first four modes in Fig. 19 to Fig. 21, it can be observed that the values at the finite element nodes fall accurately on the spatial envelope of the analytical solutions. Even for the fourth-order mode, the discrete points still perfectly coincide with the analytical curves. Concurrently, a comparison of the increasing number of elements from 16 to 48 reveals that 16 elements already possess high accuracy in capturing the peak bending moments. As the number of divided elements increases to 48, the predicted distribution profiles fully approximate the pure harmonic waves, thereby highly converging toward the analytical distribution profiles. This fully demonstrates that the proposed element can rigorously maintain the physical constraint of zero bending moments at the ends under simply-supported boundary conditions, thus validating the reliability and rigor of the numerical model.

3. Conclusion

Aiming to improve the low accuracy and inefficiency of conventional Timoshenko beam elements caused by the omission of shear force and bending moment conditions, this study proposes a new beam element formulation capable of achieving both high accuracy and efficiency, which incorporates conventionally omitted force conditions of shear forces and bending moments, and resolves the computational inefficiency at higher modes.

We propose a novel 2-node 8-DOF Timoshenko beam element. The nodal degrees of freedom for this new element are formulated on basis of the beam's transverse displacement, cross-sectional rotation, and their corresponding derivatives, in which the derivatives respectively correspond to the shear force and bending moment. For the transverse displacement and the cross-sectional rotation of the Timoshenko beam element, novel displacement field expressions are proposed based on cubic Hermite interpolation functions through the exact constitutive relationships between the internal forces and the displacement derivatives, where the proposed beam element employs nodal degrees of freedom that include internal forces. However, this element is fundamentally different from the classic mixed elements. The distinction lies in the fact that the internal forces are not independently interpolated and solved via a mixed variational principle. Instead, the variational formulation used to derive the presented theory of the proposed element is a single type, i.e. the displacement type.

Numerical results demonstrate that the proposed element is applied to uniform Timoshenko beam and beam with linear variable cross-section. For different types of boundary conditions, the calculated results of natural frequencies by the proposed Timoshenko beam element exhibit exceptional agreement with both the analytical solutions and finite element values by commercial software. Notably, the present

element avoids the requirement for excessive mesh refinement while maintaining superior computational accuracy and high efficiency. In comparison with the conventional Timoshenko beam elements, although both can yield nearly identical results of the natural frequency, the relative errors of the proposed beam element is just one third or less of that of the conventional element for high mode order. This phenomenon fully demonstrates the precision superiority of the proposed element in the dynamic characteristic analysis. The mode shape of the displacement is demonstrated to be coincided with the analytical solutions. Furthermore, the distribution of the internal forces is directly solved at the nodal point location, which are highly consistent with the analytical one.

This study provides an efficient and highly accurate numerical computational methodology for the vibration analysis of Timoshenko structures, demonstrating the promising and broad prospects for modern engineering applications that demand both high precision and high efficiency. Furthermore, the predictions by the present approach are expected to serve as benchmarks for evaluating the performance of other numerical methods.

Acknowledgements This research did not receive any specific grant from funding agencies in the public, commercial, or not-for-profit sectors.

Author Contributions Conceptualization: S.B., L.D., X.X.; Methodology: S.B., L.D., X.X.; Formal analysis: L.D., X.X., S.W.; Software: X.X., D.L; Numerical simulations: S.B., L.D.; Validation: S.B., L.D., X.X.; Supervision: S.B.; Writing - review and editing: S.B., L.D., S.W..

Funding No funding was received to assist with the preparation of this manuscript.

Data Availability No datasets were generated or analysed during the current study.

Declarations

Conflict of interest

The authors declare no conflict of interest.

Ethics, Consent to Participate, and Consent to Publish declartions: Not applicable.

References

[1] Hughes T J R, Taylor R L, Kanoknukulchai W. A simple and efficient finite element for plate bending. International Journal for Numerical Methods in Engineering, 1977, 11(10): 1529-1543.

[2] Przemieniecki J S. Theory of matrix structural analysis. Courier Corporation, 1985.

[3] Friedman Z, Kosmatka J B. An improved two-node Timoshenko beam finite element. Computers & structures, 1993, 47(3): 473-481.

[4] Friedman Z, Kosmatka J B. An accurate two-node finite element for shear deformable curved beams. International journal for numerical methods in engineering, 1998, 41(3): 473-498.

[5] Oral S. A shear correction factor for bars with arbitrary cross-section. Computers & Structures, 1991, 41(5): 1013-1019.

[6] Caillerie D, Kotronis P, Cybulski R. A Timoshenko finite element straight beam with internal

degrees of freedom. International Journal for Numerical and Analytical Methods in Geomechanics, 2015, 39(16): 1753-1773.
[7] Gerlach M E, de Barros A, Huang X, et al. The analytical beam element model: novel approach for fast calculation of vibrations in electric machines. e & i Elektrotechnik und Informationstechnik, 2023, 140(2): 290-301.
[8] Zhao B, Yang R, He J, et al. Size effect on nominal flexural strength of concrete beams influenced by damage gradient. Mechanics Research Communications, 2016, 74: 45-51.
[9] Zhao B, Liu T, Pan J, et al. A stress analytical solution for Mode III crack within modified gradient elasticity. Mechanics Research Communications, 2017, 84: 142-147.
[10] Li C, Yao L, Chen W, et al. Comments on nonlocal effects in nano-cantilever beams. International Journal of Engineering Science, 2015, 87: 47-57.
[11] Li H N, Wang W, Lai S K, et al. Nonlinear vibration and stability analysis of rotating functionally graded piezoelectric nanobeams. International Journal of Structural Stability and Dynamics, 2024, 24(09): 2450103.,
[12] Song H, Li C, Qing H. Size-dependent bending and buckling analysis of piezoelectric semiconductor nanobeam based on two-phase local/nonlocal integral models: H. Song et al. International Journal of Mechanics and Materials in Design, 2026, 22(1): 48.
[13] Song Z, Zhao B, He J, et al. Modified gradient elasticity and its finite element method for shear boundary layer analysis. Mechanics Research Communications, 2014, 62: 146-154.
[14] Civalek Ö. An effective analytical method for buckling solutions of a restrained FGM nonlocal beam[J]. Computational and Applied Mathematics, 2022, 41(6): 387.
[15] Civalek Ö. Finite element formulation of metal foam microbeams via modified strain gradient theory[J]. Engineering Computations, 2023, 40(8): 2145-2168
[16] Challamel N, Wang C M, Reddy J N, et al. Equivalence between micromorphic, nonlocal gradient, and two-phase nonlocal beam theories. Acta Mechanica, 2025, 236(2): 871-902.
[17] Demetriou P, Rizzi G, Madeo A. Reduced relaxed micromorphic modeling of harmonically loaded metamaterial plates: investigating boundary effects in finite-size structures . Archive of Applied Mechanics, 2024, 94(1): 81-98.
[18] Eremeyev V, Elishakoff I. Rotary inertia effects in micromorphic microstructured beams . Mechanics Research Communications, 2024, 124: 103926.
[19] El-Borgi S, Trabelssi M, Challamel N, et al. Static bending of micromorphic Timoshenko beams. International Journal of Engineering Science, 2026, 218: 104403.
[20] Tuna M, Kirca M. Exact solution of Eringen's nonlocal integral model for bending of Euler-Bernoulli and Timoshenko beams. International Journal of Engineering Science, 2016, 105: 80-92.
[21] Karttunen A T, Romanoff J, Reddy J N. Exact microstructure-dependent Timoshenko beam element. International Journal of Mechanical Sciences, 2016, 111: 35-42.
[22] Dehrouyeh-Semnani A M, Bahrami A. On size-dependent Timoshenko beam element based on modified couple stress theory. International Journal of Engineering Science, 2016, 107: 134-148.
[23] Ziou H, Guenfoud H, Guenfoud M. Numerical modelling of a Timoshenko FGM beam using the finite element method. International Journal of Structural Engineering, 2016, 7(3): 239-261.
[24] Çelik, M., Demirkan E., Yıldırım A.F. Analytical and numerical investigation of vibration

characteristics in shear-deformable FGM Beams. J. Compos. Sci. 2025, 9, 567.
[25] Ruocco E, Reddy J N. Analytical solutions of Reddy, Timoshenko and Bernoulli beam models: A comparative analysis. European Journal of Mechanics-A/Solids, 2023, 99: 104953.
[26] Ruocco E, Reddy J N. A closed-form solution for accurate stress analysis of functionally 4graded Reddy beams. Composite Structures, 2023, 307: 116676.
[27] Xie M, Ou H, Sun J, et al. Timoshenko-EFEA model for tapered beams and its application. Archive of Applied Mechanics, 2026, 96(5): 112.
[28] Chen Z, Yang Z, Guo N, et al. An energy finite element method for high frequency vibration analysis of beams with axial force. Applied Mathematical Modelling, 2018, 61: 521-539.
[29] Skrinar M. Computational analysis of multi-stepped beams and beams with linearly-varying heights implementing closed-form finite element formulation for multi-cracked beam elements. International Journal of Solids and Structures, 2013, 50(14-15): 2527-2541.
[30] Bazoune A. Free vibration frequencies of a variable cross-section Timoshenko-Ehrenfest beam using Fourier-p element. Arabian Journal for Science and Engineering, 2024, 49(2): 2831-2851.
[31] Ji P, Yin Z. Hermite Finite Element Method for Vibration Problem of Euler-Bernoulli Beam on Viscoelastic Pasternak Foundation. Engineering, 2024, 16(10): 337-352.
[32] Tang Y, Yin Z. Hermite finite element method for a class of viscoelastic beam vibration problem. Engineering, 2021, 13(08): 463-471.
[33] Gong Y. A Hermite finite element method for the vibration problem of the Rayleigh-Bishop beam. Journal of Applied Analysis & Computation, 2025, 15(2): 1134-1145.
[34] Taylor R L, Filippou F C, Saritas A, et al. A mixed finite element method for beam and frame problems. Computational mechanics, 2003, 31(1): 192-203.
[35] Pian T H H. Finite element formulation by variational principles with relaxed continuity requirements//The mathematical foundations of the finite element method with applications to partial differential equations. Academic Press, 1972: 671-687.
[36] Tian Z S, Liu J S, Ye L, et al. Studies of stress concentration by using special hybrid stress elements. Int J Num Meth Engng, 1997, 40: 1399-1412.
[37] Pian T. H. H., C. C. Wu. A rational approach for choosing stress terms for hybrid finite element formulations. International Journal for Numerical Methods in Engineering, 1988, 26, (10): 2331-2343.

.

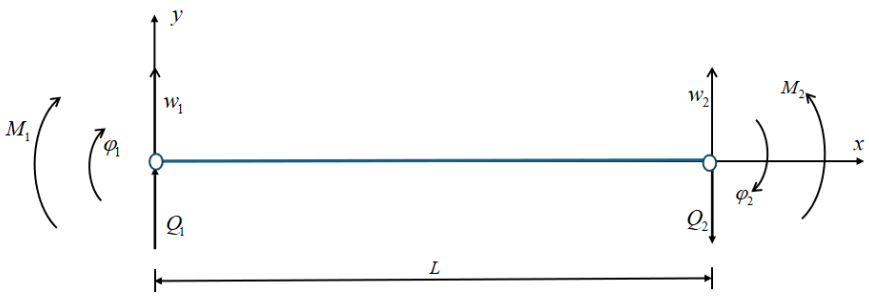


Figure 1. The present element with nodal degrees of freedom

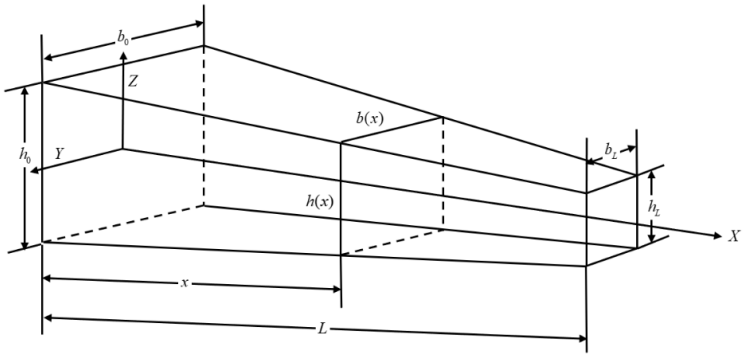


Fig. 2 Schematics of the linear variable cross-section beam

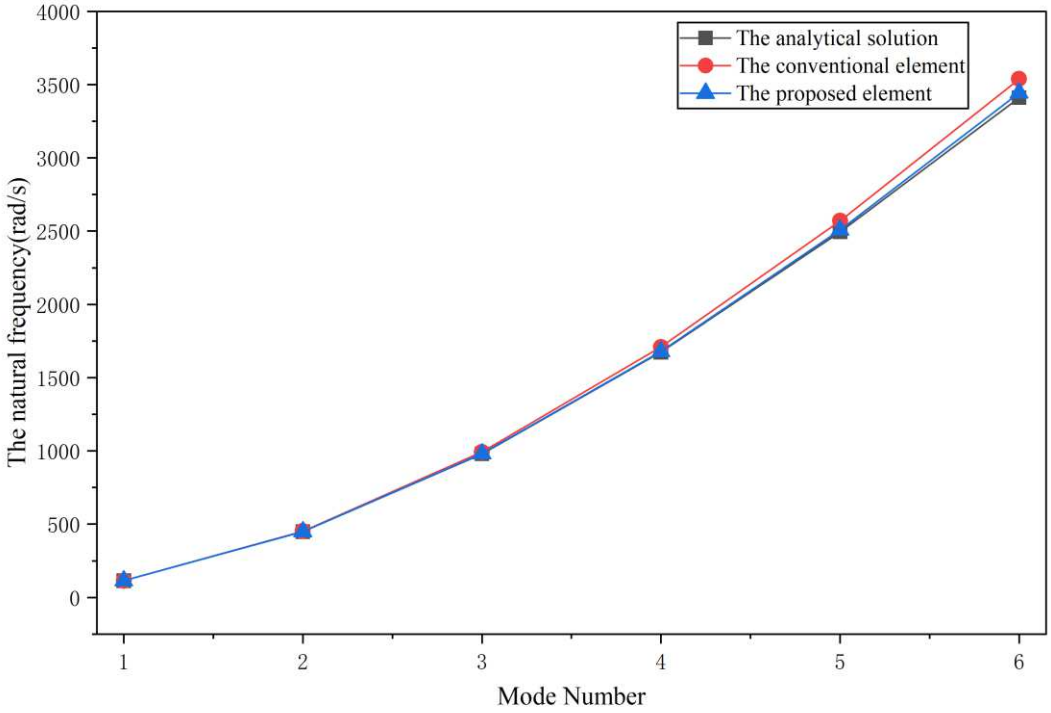


Fig. 3. Comparison of natural frequencies for a simply-supported Timoshenko beam among the three results: the conventional element, the proposed element and the analytical solution (48 elements)

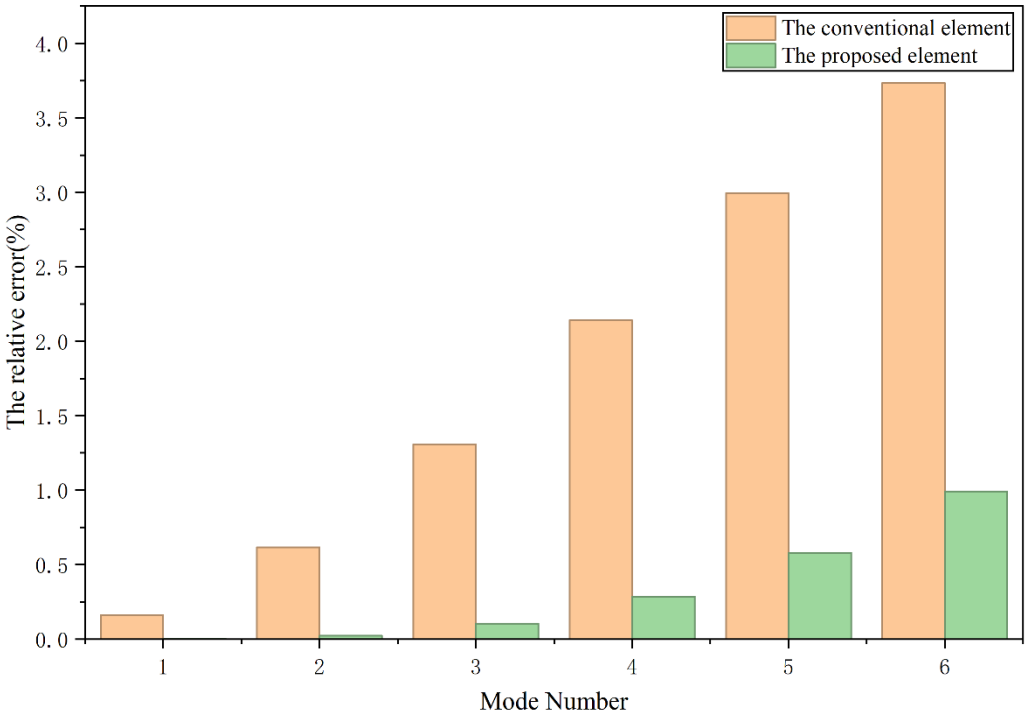


Fig. 4. Comparison of relative errors in natural frequencies for a simply-supported Timoshenko beam (48 elements)

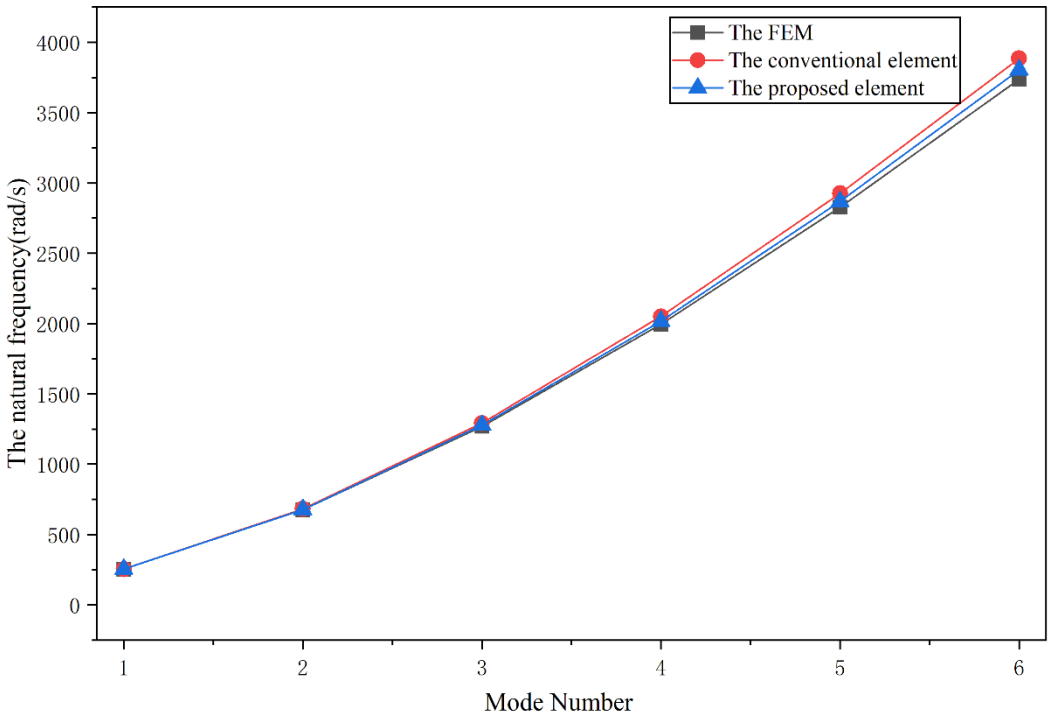


Fig. 5. Comparison of natural frequencies for a C-C Timoshenko beam among the three results: the conventional element, the proposed element and the FEM (48 elements)

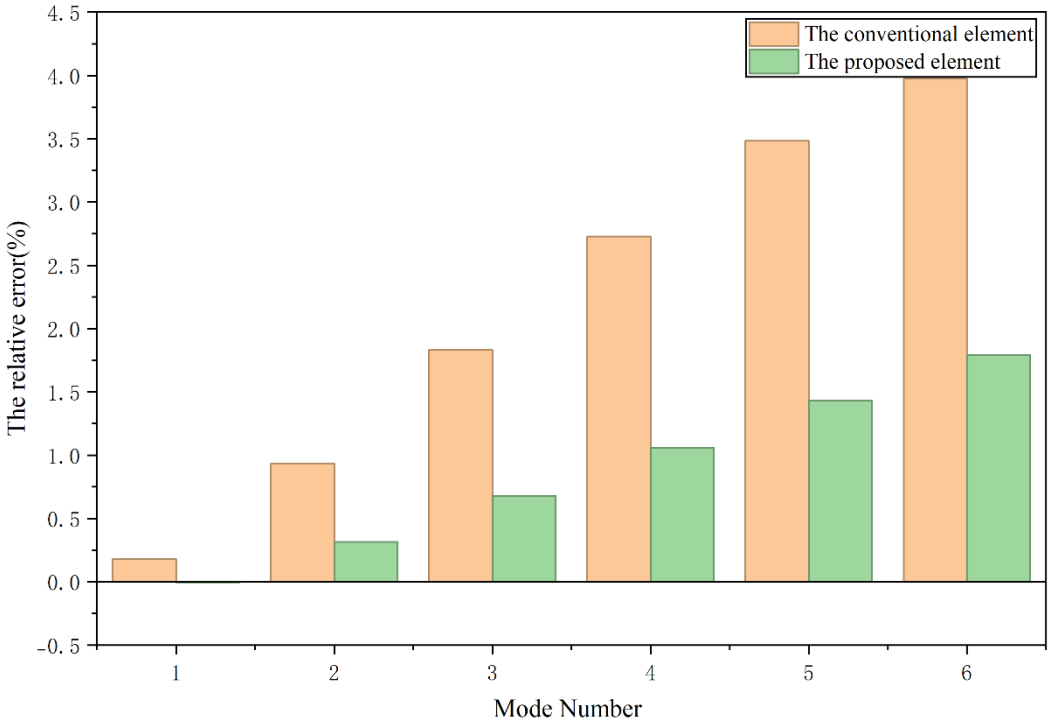


Fig. 6. Comparison of the relative errors of the natural frequencies for a clamped-clamped Timoshenko beam (48 elements)

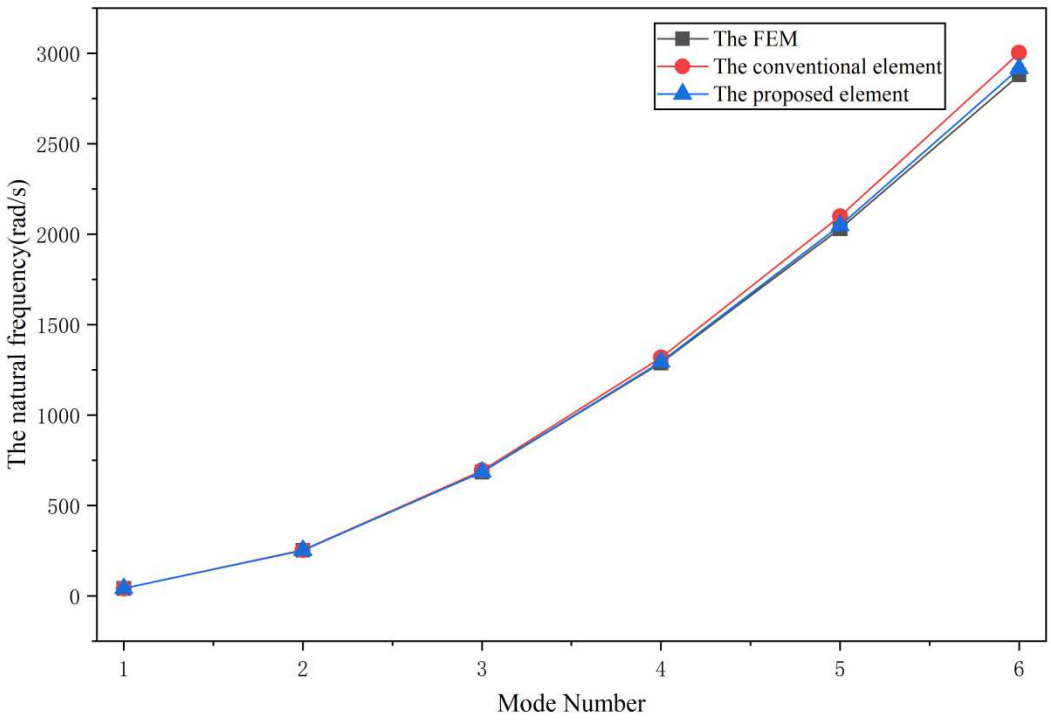


Fig. 7. Comparison of the natural frequencies for a C-F Timoshenko beam among the results by the conventional element, the proposed element and the FEM of ABAQUS (48 elements)

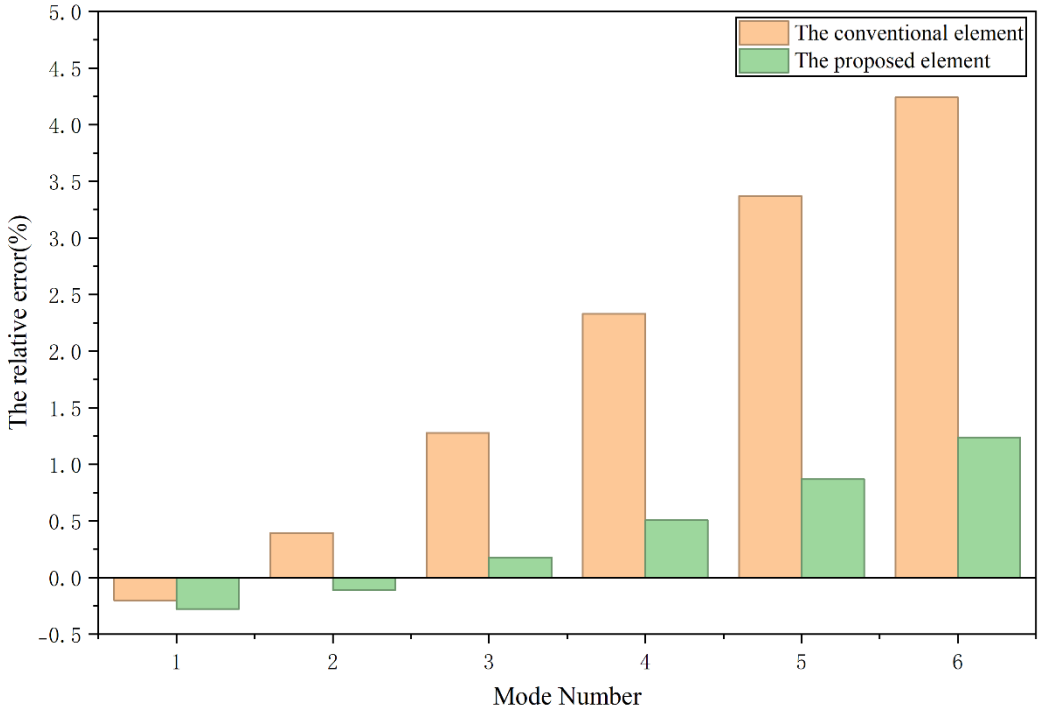


Fig. 8. Comparison of relative errors in natural frequencies for a C-F Timoshenko beam (48 elements)

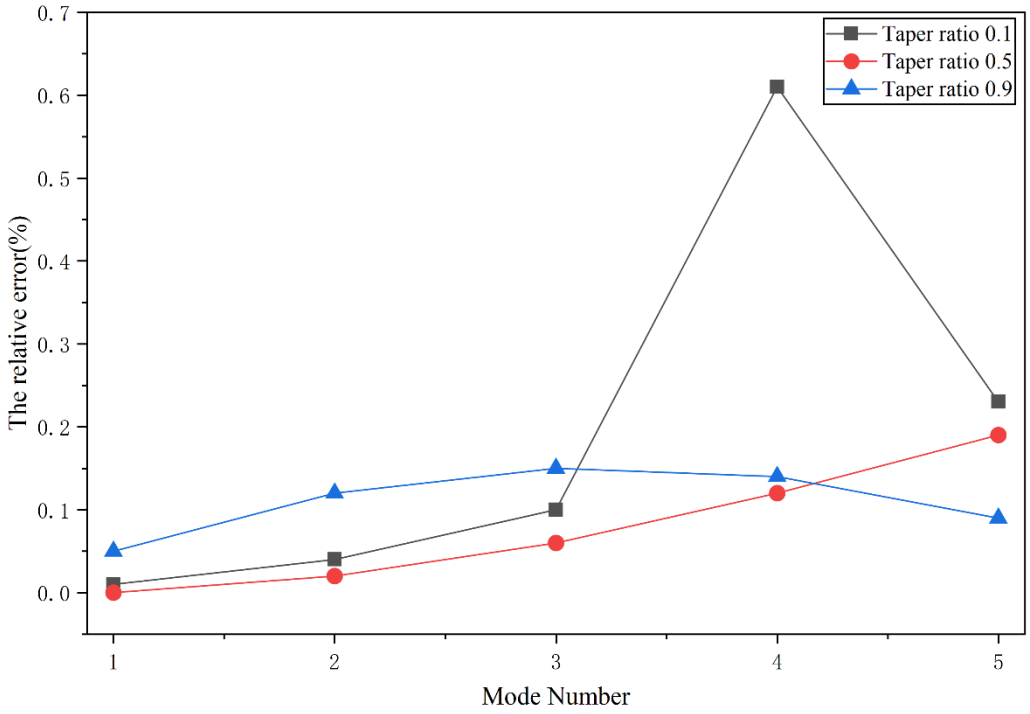


Fig. 9. Errors of the natural frequency by the proposed Timoshenko beam with a linearly variable cross-section under C-F boundary condition (48 elements)

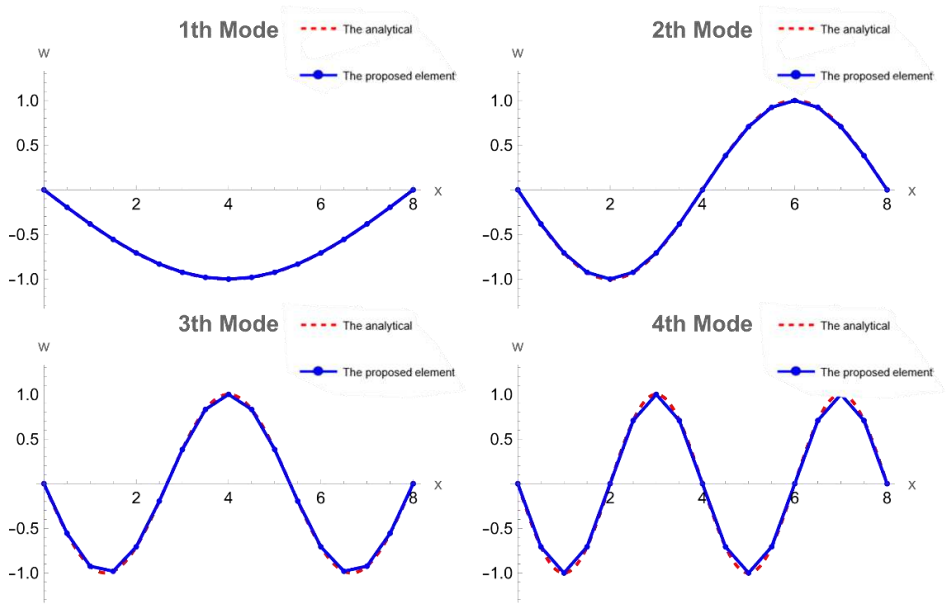


Fig. 10. The first four deflection mode shapes of a simply-supported beam (using 16 elements)

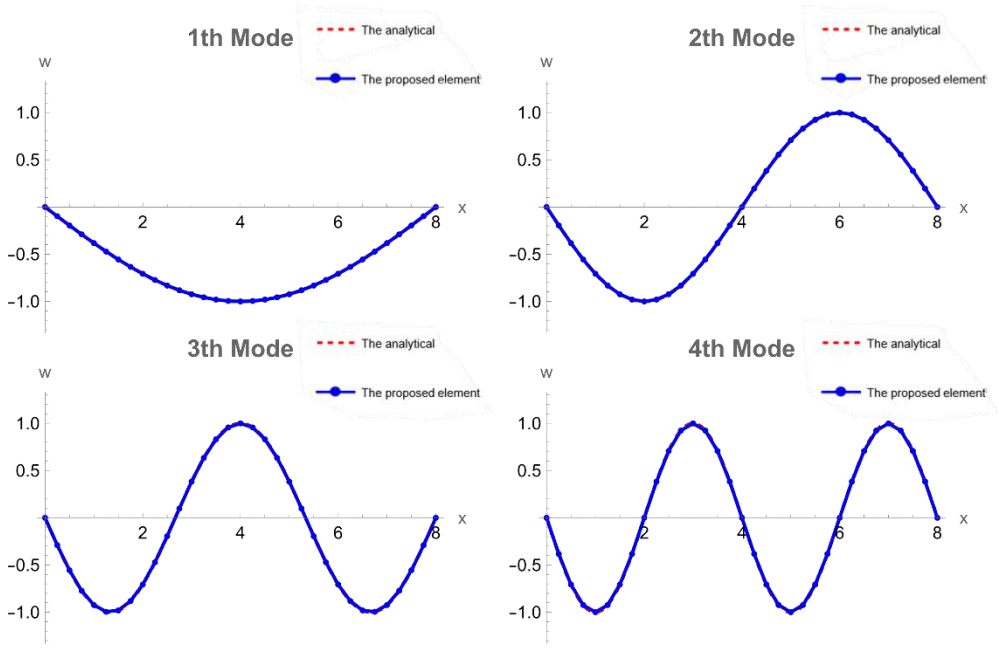


Fig. 11. The first four deflection mode shapes of a simply-supported beam (using 32 elements)

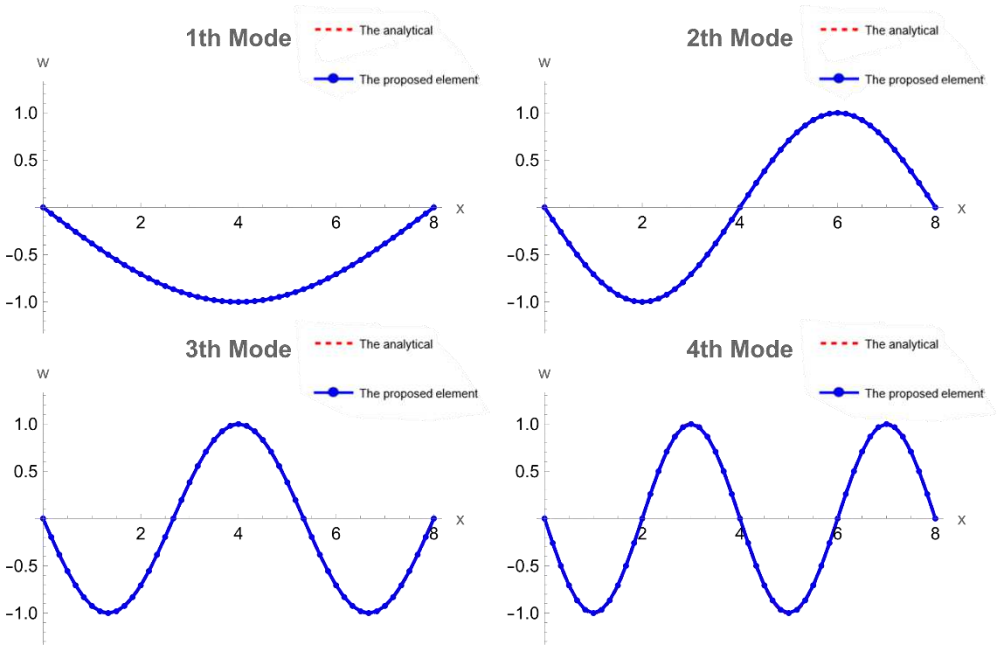


Fig. 12 The first four deflection mode shapes of a simply-supported beam (using 48 elements)

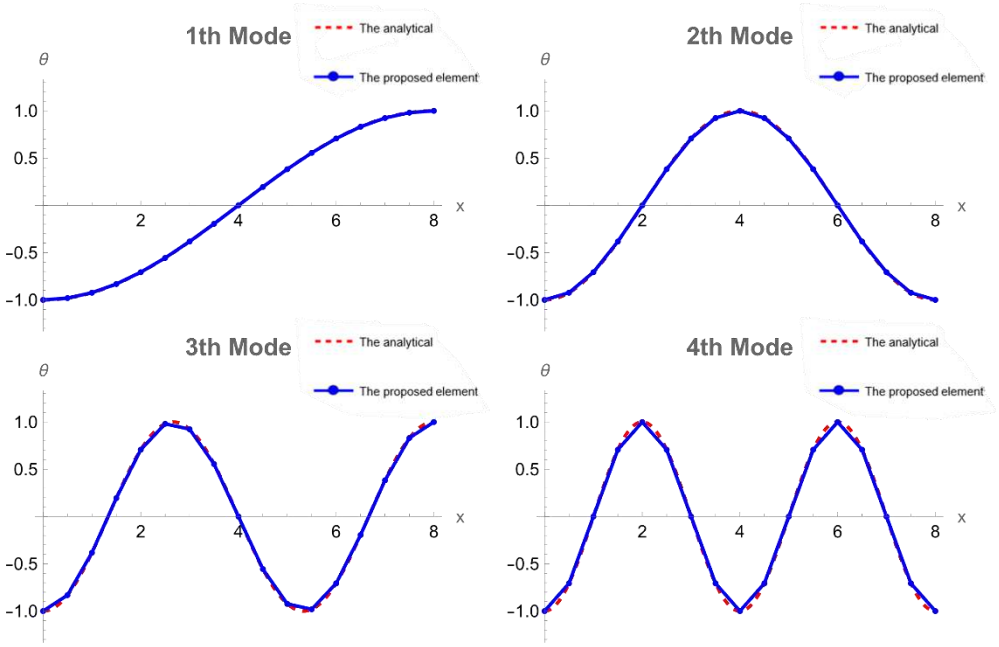


Fig. 13 The first four rotation mode shapes of a simply-supported beam (using 16 elements)

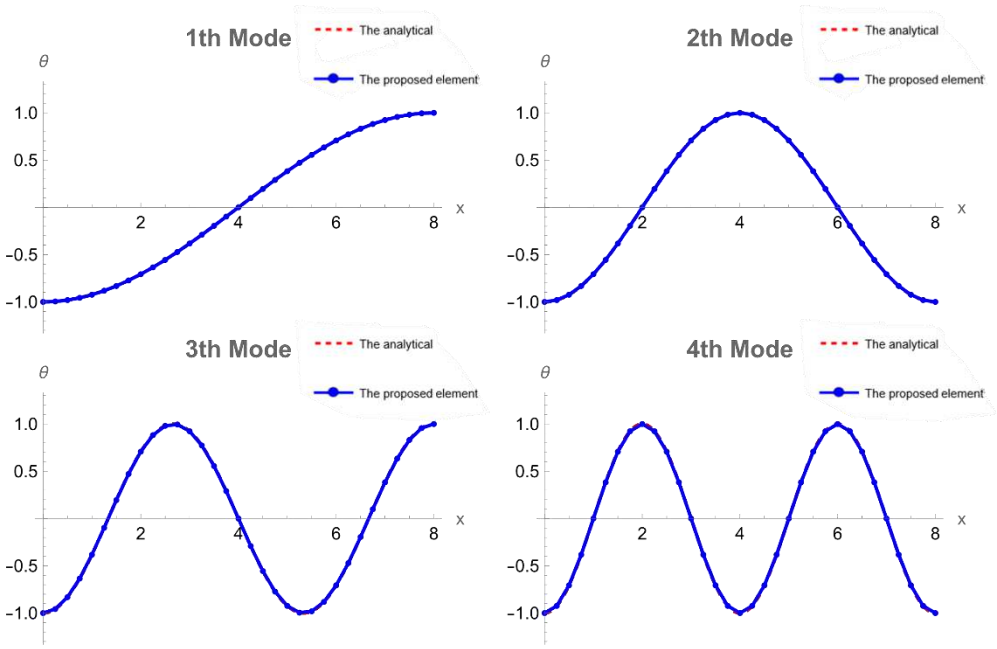


Fig. 14 The first four rotation mode shapes of a simply-supported beam (using 32 elements)

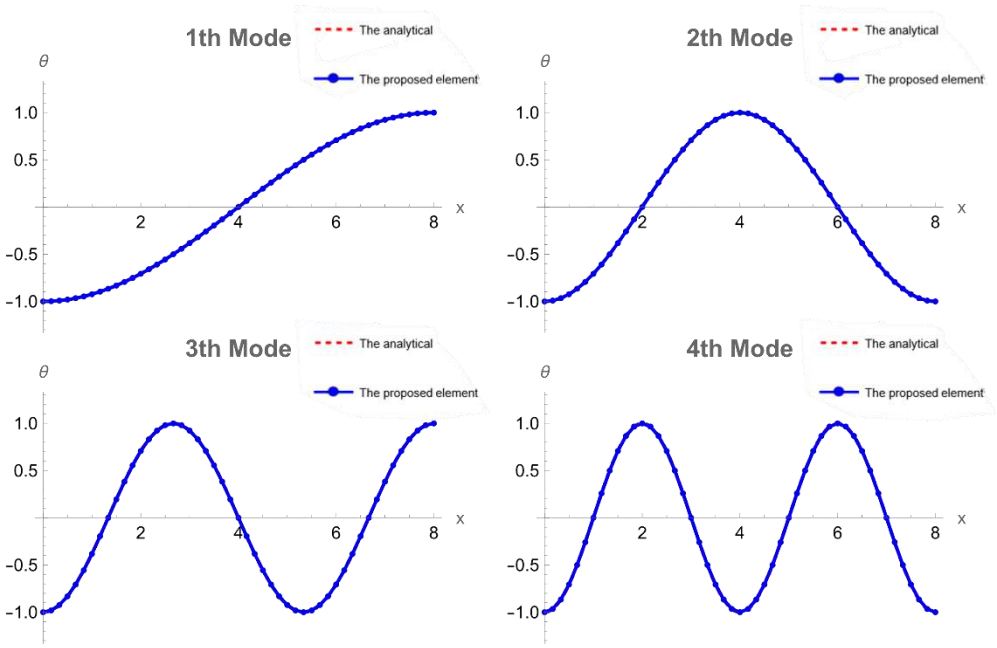


Fig. 15 The first four rotation mode shapes of a simply-supported beam (using 48 elements)

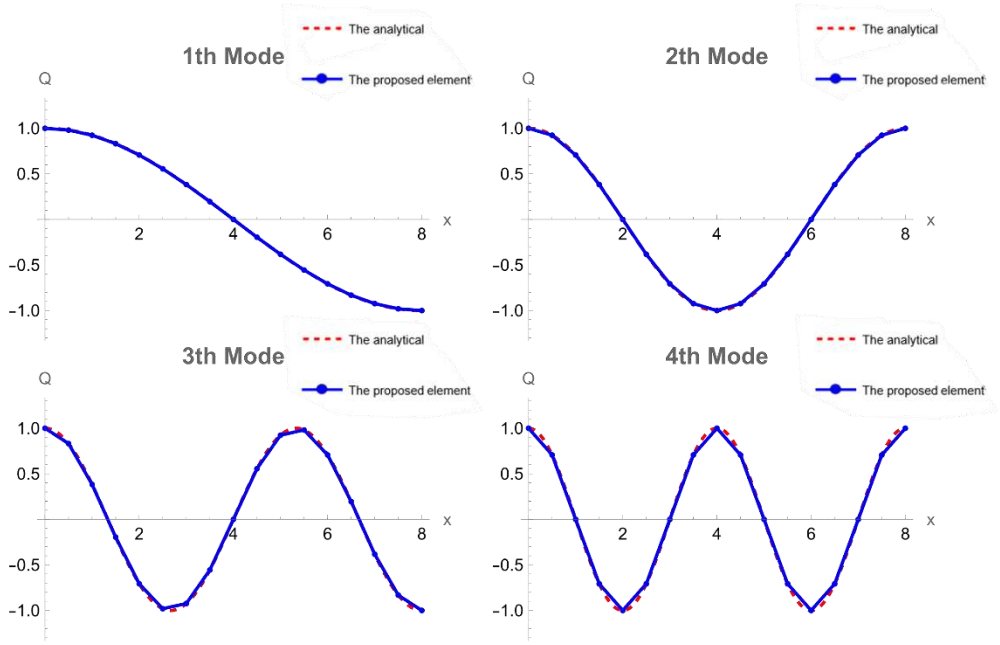


Fig. 16 The first four shear force distributions of a simply-supported beam (using 16 elements)

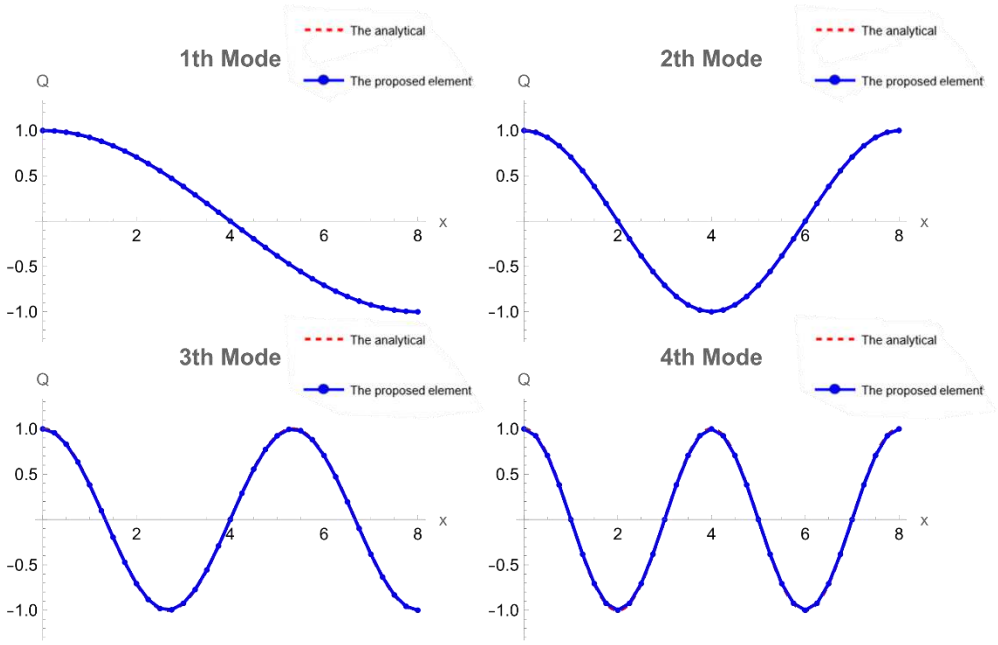


Fig. 17 The first four shear force distributions of a simply-supported beam (using 32 elements)

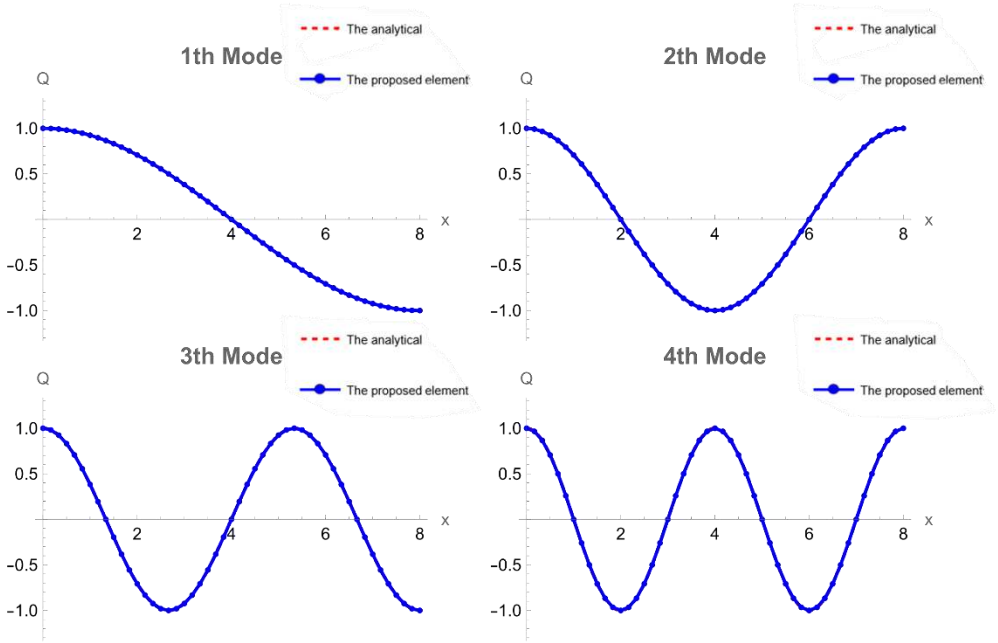


Fig. 18 The first four shear force distributions of a simply-supported beam (using 48 elements)

Figure Capitions

Fig. 1 The present element with nodal degrees of freedom
Fig.2 Schematics of the linear variable cross-section beam
Fig. 3 Comparison of natural frequencies for a simply-supported Timoshenko beam among the three results: the conventional element, the proposed element and the analytical solution (48 elements)
Fig. 4 Comparison of relative errors in natural frequencies for a simply-supported Timoshenko beam (48 elements)
Fig. 5 Comparison of natural frequencies for a C-C Timoshenko beam among the three results: the conventional element, the proposed element and the FEM (48 elements)
Fig. 6 Comparison of the relative errors of the natural frequencies for a clamped-clamped Timoshenko beam (48 elements)
Fig. 7 Comparison of the natural frequencies for a C-F Timoshenko beam among the results by the conventional element, the proposed element and the FEM of ABAQUS (48 elements)
Fig. 8 Comparison of relative errors in natural frequencies for a C-F Timoshenko beam (48 elements)
Fig. 9 Errors of the natural frequency by the proposed Timoshenko beam with a linearly variable cross-section under C-F boundary condition (48 elements)
Fig. 10 The first four deflection mode shapes of a simply-supported beam (using 16

elements)
Fig. 11 The first four deflection mode shapes of a simply-supported beam (using 32 elements)
Fig. 12 The first four deflection mode shapes of a simply-supported beam (using 48 elements)
Fig. 13 The first four rotation mode shapes of a simply-supported beam (using 16 elements)
Fig. 14 The first four rotation mode shapes of a simply-supported beam (using 32 elements)
Fig. 15 The first four rotation mode shapes of a simply-supported beam (using 48 elements)
Fig. 16 The first four shear force distributions of a simply-supported beam (using 16 elements)
Fig. 17 The first four shear force distributions of a simply-supported beam (using 32 elements)
Fig. 18 The first four shear force distributions of a simply-supported beam (using 48 elements)
Fig. 19 The first four bending moment distributions of a simply-supported beam (using 16 elements)
Fig. 20 The first four bending moment distributions of a simply-supported beam (using 32 elements)
Fig. 21 The first four bending moment distributions of a simply-supported beam (using 48 elements)